UNITED KINGDOM ATOMIC ENERGY AUTHORITY SRD/ HSE/ R 410

SRD/HSE/R 410

SAFETY AND RELIABILITY DIRECTORATE

DISCHARGE OF LIQUID AMMONIA TO MOIST ATMOSPHERES – SURVEY OF EXPERIMENTAL DATA AND MODEL FOR ESTIMATING INITIAL CONDITIONS FOR DISPERSION CALCULATIONS

C. J. Wheatley

Price £ 5.00 C.10

HEALTH AND SAFETY EXECUTIVE

April 1987

SRD R410

UNITED KINGDOM ATOMIC ENERGY AUTHORITY
SAFETY AND RELIABILITY DIRECTORATE

Discharge of liquid ammonia to moist atmospheres – survey of experimental data and model for estimating initial conditions for dispersion calculations

by

C. J. Wheatley

SUMMARY

A mathematical model is proposed for estimating concentrations near an accidental release of liquefied ammonia from a hole in a tank wall or from a severed pipe. Three quantities are particularly important for hazard assessment:

- the discharge rate;
- the fraction of liquid which rains out of the two-phase jet; and
- the amount of dilution with air up to a point where atmospheric mixing or gravitational effects become important.

As well as these, the model includes the chemical interaction of ammonia with atmospheric water vapour: this influences the mixture density and thus the rate of dilution in a subsequent heavy-gas dispersion phase.

Part I is a survey of relevant experimental data. In Part II, the mathematical details of the integral model are developed in sufficient detail for implementation in a computer code.

April 1987

ISBN No. 0-85-356220-2

CONTENTS

PART I

A SURVEY OF EXPERIMENTAL DATA

1. INTRODUCTION

Ammonia (NH_3) is commonly used in the chemical process industry throughout the United Kingdom. It is stored in bulk in liquid form under pressure at ambient temperatures, or refrigerated at its boiling point, or at intermediate temperatures. It is toxic and consequently it is essential to ensure that it does not endanger the public should it be accidentally released.

A number of types of release might occur. These include release from a hole in the vapour space of the tank, release from a hole below the liquid level and catastrophic failure of the tank. The first is much less hazardous than the second and the third is very unlikely to occur. Only the release from a hole below the liquid level is considered here.

Many models exist for calculating dispersion of NH_3 in the atmosphere and others are under development. However, no models exist for calculating the behaviour of two-phase jets of NH_3 at and close to the point of release. Such models are nevertheless essential to provide initial values for dispersion calculations. The purpose of the present work is therefore to suggest a model for making estimates of NH_3 concentrations near to a release of liquefied NH_3 from either a hole in a tank wall or a severed pipe.

Three quantities in particular are needed. These are:

- the discharge rate;
- the amount of rain-out of liquid from the jet of NH_3; and
- the amount of dilution with air up to the point at which atmospheric processes become dominant in causing dilution.

The rate of dilution of NH_3/air mixtures is known to depend on the mixture density. This in turn depends on the amount of moisture in the atmosphere amongst other things. So, the presence of moisture will be taken into account in calculating the dilution of the NH_3 jet.

Experimental data on discharge of two-phase jets of NH_3 will be surveyed in this Part. Development of a model is left to Part II. Special attention will be paid to measurements of discharge rates, the drop size at the outlet, the rain-out fraction from the jet, and the density and rate of dilution of the jet.

2. A SUMMARY OF THE EXPERIMENTS AND RESULTS

2.1 Introduction

In a thorough search of the literature, a number of experimental studies of two-phase discharge of ammonia have been found. In the following sub-sections results relevant to the present problem will be summarised.

2.2 Experiments at Boissise-la-Bertrand, France, 1967

These experiments were done by a French consortium and have been reported by Resplandy.[35] Their purpose was to ascertain what safety measures were required for industrial plant and its environment.

Several experiments were done involving pressurised release of ammonia from below the liquid level from a tank. During the experiments, attention focussed on how quickly the ammonia jet dispersed and what measures could be taken to mitigate the effects of the ammonia. Measurements were made of the jet near to the point of release. (Release of pressurised ammonia from above the liquid level and the behaviour of liquid ammonia in the open were also studied. These experiments will be ignored.)

The source of the ammonia was a 15 tonne pressurised tanker. The temperature of the ammonia in the tank was not recorded. The pressure in the tank was stated to be six bars. It was

not stated whether this was measured or estimated. At six bars the ammonia temperature would have been 15°C which is comparable to the recorded ground temperatures of 13 - 17°C. The air temperature was not recorded but the relative humidity was stated to be 85%. The wind speed varied between 0 - 3 m s^{-1}.

Ten experiments were done during which liquid ammonia was discharged through a 50 mm diameter pipe at ground level pointing vertically upward. The amount of ammonia released in each experiment was in the range 200 - 300 kg for a period of ~ 1 minute per experiment. An opaque white two-phase jet was formed at the point of discharge. No substantial increase in the jet diameter close to the outlet due to flashing can be seen from published photographs. The drop size in the jet was not measured but the liquid was stated to be pulverised. The velocity of the jet at the source was not measured. No liquid ammonia was observed to rain-out. The momentum of the jet was sufficient to cause it to rise into the air by 20 metres. It subsequently fell back to the ground away from the point of release. Clearly, the jet was denser than air.

The amount of air entrained into the jet close to the source was not measured. However, a geometric measurement of the jet can be made from a published photograph. The jet half angle, β, was found to be 5°. This gives an effective entrainment coefficient of 0·044 according to the formula $\alpha = \frac{1}{2} \tan\beta$. Measurement at ground level 40 m from the point of release gave a peak ammonia concentration of 1·4% by volume and at 60 m gave a peak ammonia concentration of 0·5% by volume.

In experiments liquid ammonia was discharged through a 25 mm diameter pipe. The amounts discharged were 110 kg in 60 seconds and 113 kg in 65 seconds. In the second of these emissions the jet was directed downward into a stainless steel container whose bottom was 15 cm below the outlet. In this case 77% of the ejected ammonia was collected as liquid in the container. However, it should be noted that the eventual level in the container was 40 cm and so the jet was bubbling through liquid for a substantial period of time.

2.3 Experiments at Mourmelon, France, 1968

These experiments were a follow-on to the experiments done at Boissise-la-Bertrand in 1967 and also by Resplandy.[35] Their purpose was to characterise the plume of ammonia downwind of the release point.

The source of ammonia was a 15 tonne pressurised tanker. The pressure in the tank was stated to be six bars. It was not stated whether this was measured or estimated. The air temperature was not recorded. The relative humidity was measured and varied between 95% at the start of the experiments at 0800 h in the morning and 80% at the end of the experiments at mid-day. The wind speed varied between 0 - 3 m s^{-1}.

Eleven experiments were done with liquid ammonia discharged through a 50 mm diameter pipe. The pipe was directed both vertically and horizontally. Discharge rates were similar to those at Boissise-la-Bertrand. Observations were made of the behaviour of the plume downwind of the jet.

2.4 Experiments done by Unie van Kunstmest Fabrieken bv, Holand, 1972

These experiments were done by J. W. Frenken in 1972, and have been briefly described by Blanken.[4] The ammonia used in the experiments was stored under a pressure of 3·5 bars and at 0°C. The ambient temperature was − 10°C. The humidity was not recorded. The windspeed was 2 - 3 m s^{-1}. The ammonia was emitted from below the liquid level in the tank from a short nozzle with an exit diameter of 8 mm.

Two experiments were done: in one, the jet pointing horizontally 1800 mm above the ground and perpendicular to the wind; and in the other the jet pointed vertically downward 2000 mm above the ground. Each experiment lasted one minute. The object of the experiments was to measure the amount of liquid ammonia collected on the ground: this was 5·5 kg and 27·3 kg for the two experiments respectively. In both cases the mass of ammonia discharged was 38·4 kg. No measurements were made of the drop size at the orifice.

The jet at the source was reported to expand over a distance of 20 - 30 mm due to flashing of ammonia outside the nozzle: however, the increase in diameter cannot be discerned from the published photographs. Flashing at the outlet implies that the ammonia was superheated at this point. This may be explained by assuming the NH_3 was liquid in the pipe. The discharge rate is consistent with this assumption. The jet subsequently entrained air. The jet half-angle for the horizontal release can be measured from the photograph and is found to be 5 - 7°. This gives an entrainment coefficient of between 0·044 and 0·061. No measurements of ammonia in air concentrations were made.

2.5 Experiments by Imperial Chemical Industries, England, 1974

These experiments have been reported by Reed.[34] Their purpose was to assess the effectiveness of bunds for containing leaks of liquid ammonia stored under pressure.

Two series of experiments were done. In the first series, the lid of a pressurised container was suddenly released to simulate catastrophic failure of a vessel; these experiments will not be considered further here. In the second series, ammonia was discharged through a 1 mm orifice via a pipe connected to a pressurised tank of ammonia below the liquid level. The pressure and temperature of the tank contents was 6·5 bars and 16°C respectively. The air temperature and humidity were not recorded.

A number of experiments were done with the orifice held at 1 m above ground level at various angles. When it was horizontal or pointing slightly upward an opaque aerosol was formed and no rain-out of ammonia was observed. When it pointed slightly downward directed at a metal tray on the ground, a small fraction of the discharged ammonia collected in the tray. No other observations were made.

2.6 Experiments done by Unie van Kunstmest Fabrieken bv, Holland, 1980

In these experiments by Blanken,[4] the ammonia was stored at 13·4 bar, implying a temperature of 38°C. Liquid ammonia was released into atmospheres of pure ammonia and moist air through a capillary tube of internal diameter 2 mm and length 100 mm.

The purpose was to investigate the drop size in the jet. Only qualitative results were recorded. In the ammonia atmosphere, the jet was transparent and liquid separated out of the jet and collected on the floor of the containing vessel. In moist air the jet was opaque and no liquid was collected. It was assumed that the initial ammonia aerosol quickly vaporised when diluted with air and so it was concluded that the opaqueness was caused by condensation of water, forming an aqueous ammonia aerosol.

2.7 Experiments at Landskrona, Sweden, 1982

These experiments were done by the Swedish National Defence Research Institute and have been reported by Nyrén et al.[27] A summary of the experiments and comparison with a pipe flow model have been given by Nyrén and Winter.[26]

The ammonia was stored in a commercial 1·4 tonne tank at ambient temperature. The temperature and pressure in the tank were recorded throughout each experiment, and were typically 9°C and six bars respectively. The air temperature and humidity were also recorded for each experiment being typically 8°C and 42%. The wind speed was 13 m s^{-1}. Ammonia was supplied from the tank from below the liquid level through a pipe with internal diameter varying between 32 and 40 mm. Six experiments were done with a pipe length of 2 m and five with a length of 3·5 m. The pipe was horizontal at 2 m above ground level.

The purpose of the experiments was to measure discharge rates for a flashing flow of ammonia and compare them with a theoretical model. Measurements were therefore made of the mass flow rate and the exit pressure. Photographs were also taken of the jet. Each experiment lasted 60 - 90 seconds. In all but four of the experiments the pressure in the tank varied strongly. Of the

remaining experiments the mass flow rate was typically 2 · 2 kg s^{-1} and the exit pressure was typically 2 · 2 bars. Constriction in the discharge path caused the flow to be choked within the pipe. Comparisons with a model for the pipe flow suggest that the flow was homogeneous and in equilibrium.

The jet was opaque and denser than air causing it to sink and reach the ground after 6 - 10 m. No rain-out was observed. Since the flow was under-expanded at the outlet, the ammonia would have flashed causing an increase in diameter of the jet close to the outlet. This, however, cannot be resolved from the photographs, which were taken a long distance away to show the jet as a whole. Entrainment of air into the jet caused its diameter to increase. The jet half-angle close to the source is about 5° from published photographs, giving an effective entrainment coefficient of 0 · 044.

2.8 Experiments at Frenchman Flat, USA, 1983

These experiments were done by Lawrence Livermore National Laboratories on behalf of the US Coast Guard and the Fertiliser Institute at the US Department of Energy's Nevada Test Site. Preliminary results of the experiments have been reported by Koopman et al[19] and more detailed information is given in Goldwire.[13]

The ammonia was stored in two 36 m^3 road tankers at ambient temperature. It was fed via a 6-inch internal-diameter pipe about 100 m to the release point where it discharged into the atmosphere through an orifice plate chosen so that the ammonia remained liquid upstream. The size of the orifice has not been published. The ammonia was pressurised with nitrogen and an automatic valve held the flow rate constant during each experiment. The temperature of the ammonia in the pipe was measured. The discharge took place horizontally, 1 m above ground level in the direction of the wind. Ambient weather conditions were recorded but only the wind speed has yet been reported, being typically 5 - 7 m s^{-1}. The ambient temperature however would have been typically 30 - 35°C for the time of year.

The purpose of the experiments was to study the dispersion of ammonia in the atmosphere and in particular to study the effects of the aerosol on the plume.

Four experiments were performed, with release rates ranging between 7 and 10 m^3 per minute. The total liquid volume released varied between 15 and 60 m^3. The ammonia flashed rapidly on emerging to the atmosphere and formed an opaque plume. The diameter after flashing is estimated to be 1 - 2 m from photographs, much greater than the source diameter. The effects of the source (i.e. a large speed of travel relative to the wind speed) persisted to 100 m. No rain-out of ammonia was seen in three of the trials. In the fourth trial a liquid pool was formed but it contained only about 10% of the total amount discharged.

The ammonia formed a denser than air mixture with air, apparent from the formation of a low-lying spreading cloud. It started to spread very close to the release point but this is probably because the outlet was relatively close to the ground in relation to the cross-flow dimensions. Spreading due to gravity is clearly seen at about 20 m and beyond. Maximum gas concentrations in the plume as a function of distance downwind are given in Table 1. The aerosol persisted to large distances downwind, well beyond 100 m, but no detailed results have yet been published.

TABLE 1

Maximum gas concentrations in plume (volume %)

Test	Distance from source			
	100 m	800 m	1450 m	2800 m
2	9%	1 · 4%	> 0 · 05%	-
3	9%	1 · 6%	-	0 · 22%
4	10%	1 · 6%	-	0 · 53%

3. CONCLUSIONS

The measurements in many of the experiments were extensive enough for quantitative testing of models for the discharge and dilution of liquefied ammonia. This applies particularly to the experiments reported by Resplandy (Section 2.2), by Nyrén et al (Section 2.7) and by Koopman et al (Section 2.8). Indeed, the experimental results of Nyrén et al[27] have been compared with a model for calculating the discharge rate of superheated ammonia (Nyrén and Winter)[26] and preliminary results from the experiments by Koopman et al[19] have been compared with dispersion models. The purpose here is to draw broad conclusions about the behaviour of liquid ammonia discharges to assist the development of a model. Detailed comparisons with the data are left for the future.

Most of the experiments have been concerned with release of pressurised ammonia at ambient temperatures from a pipe with the following broad conclusions. The flow in the pipe is two-phase and choked. There is indirect evidence to suggest the flow is homogeneous* and in equilibrium. Flashing occurs at the outlet but it does not result in a substantial increase in diameter of the flow. This could be because the overpressure at the outlet caused a high exit velocity, though this was not measured in any of the experiments. No rain-out of the liquid fraction occurs if the jet does not impinge on a solid surface. No quantitative results are available for the degree of rain-out if impingement does occur. (The results reported by Blanken where rain-out occurred in a pre-existing ammonia atmosphere are not relevant.) Close to the outlet the jet entrains air with an effective entrainment coefficient of about 0·04. This is smaller than values typically quoted for homogeneous momentum jets which are usually about 0·08. An explanation of this will be given in Part II Section 5. In all the experiments the ammonia jet exhibited the effects of gravity some distance away from the point of release. The ammonia vapour in all cases was opaque over substantial distances because of the presence of aerosol.

The experiments at Frenchman Flat were a simulation of the release of pressurised liquid ammonia through a tank wall rupture. In this case the flow was liquid. Flashing occurred at the outlet resulting in a large increase in diameter of the flow. No rain-out occurred except where the jet was in contact with the ground where a small amount of deposition occurred. Rapid onset of spreading and gravity effects were observed. The ammonia vapour was opaque for substantial distances downwind because of the presence of aerosol.

The experiments by Unie van Kunstmest Fabrieken bv in 1972 simulated semi-refrigerated releases of liquid ammonia. The main results relate to rain-out. With the jet initially horizontal, 14% of the total release was collected on the ground. This compares with an estimated initial airborne liquid fraction of roughly 90%, and so rain-out is not significant. However, when the outlet was pointed downward so that the jet impinged on the ground, the rain-out fraction was 71%. The discharge rate is consistent with liquid flow in the pipe, but this in itself is not a useful result since the pipe length was not published. For the horizontal release, the effective entrainment coefficient was about 0·05 which, like that for the pressurised release from a pipe, is smaller than typical values for homogeneous momentum jets.

Overall, valuable results have been obtained which enable the ingredients of a model for discharge rates, flashing, rain-out and entrainment to be assembled. For discharge rates a treatment is required for both liquid and homogeneous equilibrium flows. In most cases the flow is superheated at the outlet and may be choked: this will have an effect on the speed and diameter of the flow and also on the heat available for flashing. A treatment for the behaviour at the outlet is, therefore, required.

Rain-out does not occur for free jets of pressurised ammonia, but some does occur for semi-refrigerated ammonia. No experiments are known for releases of refrigerated ammonia. It is therefore necessary to estimate the drop size at the outlet for refrigerated and semi-refrigerated releases in order to ascertain whether the drops will fall rapidly out of the jet.

Close to the outlet the rate of dilution can be estimated by assuming that the ammonia jet behaves as a homogeneous momentum jet, but with a lessened effective rate of entrainment.

**This conventionally means in the present context that the liquid and vapour velocities are the same.*

The density of a jet will be affected by the observed persistence of aerosol, caused by the presence of moisture in the entrained air: this will be important in calculating the effects of gravity which are observed before the jet slows to the wind speed. Details of the model developed are given in Part II.

PART II

A MODEL FOR ESTIMATING INITIAL CONDITIONS FOR SUBSEQUENT ATMOSPHERIC DISPERSION CALCULATIONS

1. INTRODUCTION

A model is required for estimating the behaviour of a release of liquefied NH_3 in order to provide initial conditions for atmospheric dispersion calculations. Part I of this report was devoted to a survey of experimental data on NH_3 discharge with the aim of establishing the principal ingredients of such a model. The purpose here is to develop the details of the model sufficient for its implementation in a computer code. Four main aspects will be considered in the following sections. These are:

- the estimation of discharge rates;
- flashing at the outlet;
- whether rain-out occurs; and,
- entrainment of air.

Ancillary details are left to the appendices.

Steady-state flow is assumed throughout. Broadly this requires the outlet area to be sufficiently small that conditions in the tank, pipe and at the outlet are changing only slowly with time. A schematic diagram of the discharge and its various stages downstream is shown in Fig. 1. The variables used in the following sections have subscripts which relate to the numbered stages on the figure.

2. DISCHARGE RATES

It is important to determine the discharge rate because it determines both the mass flux of NH_3 in the ensuing plume and the speed of the flow at the outlet. The latter is relevant both to the concentrations of NH_3 in the plume and also to the break-up of liquid into drops at the outlet. A brief survey will be given of previous work on the difficult problem of estimating flow rates of superheated fluids and then equations will be developed for the flow rate of NH_3 for a number of types of flow.

2.1 Survey of previous work

There are three main types of flow of a superheated fluid to an outlet. First, the fluid may remain liquid and so be superheated at the outlet. This results in relatively large discharge rates but only applies if the flow path is short, as would be the case for discharge via a tank wall rupture or via short pipes. For example, liquid flow has been observed by Benjamin and Miller[3] for superheated water. Secondly, the fluid flow to the outlet may be a two-phase mixture with the liquid and vapour phases in thermodynamic equilibrium. The flow can be choked at the outlet in which case it will be superheated. Equilibrium flow results in lessened discharge rates compared to liquid flow and occurs when the flow path to the outlet is long. For example, this has been shown to be so for NH_3 by Nyrén and Winter[26] (see Part I, Section 2.7). Thirdly, there is a continuum of cases for which the flow to the outlet is two-phase but the liquid and vapour phases are not in thermal equilibrium; these have intermediate flow rates.

A considerable amount of experimental and theoretical work has been done on discharge of superheated water, and reliable models have been developed. However, the phenomenology in these models may be specific to water. This particularly applies to criteria for deciding between the three categories of flow described above.

A number of models have been published for calculating discharge rates of superheated fluids other than water. Recent examples are van den Akker and Bond,[1] Cremer and Warner,[7] Duiser,[9] Jones and Underwood,[17] Morris and White[24] and Nyrén and Winter.[26] References to earlier models are given by Perry[30] and Lees.[21]

None of these authors has given a satisfactory criterion for distinguishing between the three types of flow. For example, Nyrén and Winter[26] introduce a phenomenological 'disequilibrium' parameter and fail to specify how it should be determined. Cremer and Warner[7] use results for

water without modification. They assume the flow is in equilibrium if the flow-path length-to-diameter ratio, L/D, is greater than 12, liquid if L/D is less than 2 and interpolate between the discharge rates for the two cases for intermediate values of L/D. This model has been criticised by Fletcher and Johnson[12] who show experimentally using superheated Freon 12 that, while L is an important parameter, L/D does not correlate the results. This has also been discussed by van den Akker and Bond.[1] Based on the work of Henry[15] and Henry and Fauske[16] for water, Morris and White[24] assume that if the equilibrium quality (mass fraction of vapour) is greater than 0·14 then the flow is equilibrium. This seems unsatisfactory since the type of flow is then predicted to be largely independent of the path length.

A criterion for deciding between liquid or equilibrium flow has been proposed by Edwards[10] for water; because of its fundamental approach, this should be applicable to other substances. The rate controlling process for establishment of thermal equilibrium is assumed to be heat transfer from the bulk fluid to the surface of bubbles nucleated up-stream. Edwards then calculates the critical flow rate of two-phase water discharges in terms of the time scale with which thermal equilibrium is achieved in the flow. It is assumed in the theory that there is a sufficient density of nucleation sites that the rate of (heterogeneous) nucleation is not the controlling factor. Clearly, if this is so then the diameter of the flow path is irrelevant. Results from this theory compare well with experiment.

In view of these uncertainties, only the two limiting types of flow are considered further here. The experimental data reviewed in Part I provides guidance on which model to use in a number of cases. It has recently been suggested by Fauske[11] that the choice between these two flow types can be made according to the length of pipe alone: if L is less than 10 cm then the flow is liquid; otherwise the flow is equilibrium. It is not clear how valid this is for varying conditions of storage, different substances or different pipe surfaces. It is consistent with the experiments reviewed in Part I and is adopted in our model, however, where uncertainty exists it is recommended that the conservative option is chosen. Clearly, this uncertainty is not altogether satisfactory since NH_3 concentrations close to the outlet are strongly dependent on which model is chosen, as discussed by Wheatley.[40]

2.2 Simple methods for liquid and two-phase equilibrium flows

For discharge of a superheated fluid in general, a formula for the outlet flow speed, V_4, can be derived by integrating Euler's equation along the flow path, giving:

$$\tfrac{1}{2}\, V_4^2 = \alpha_P^2 \left(\int_{P_4}^{P_2} v \, dP + gh \right). \qquad \ldots (1)$$

α_P is a phenomenological discharge coefficient which accounts for non-ideality of the flow (for example, contraction at the inlet to the pipe or orifice). Perry[30] gives values for α_P of 0·6 for a thin-walled orifice ($L/D \leqslant 1$) and 0·8 for a pipe ($L/D \geqslant 1$). P_2 is the pressure in the static fluid in the tank at the height of the outlet, P_4 is the pressure at the outlet (which will be greater than ambient pressure if the flow is choked) and v is the specific volume of the fluid (i.e. reciprocal of density); g is the acceleration due to gravity and h is the height difference between the inlet and outlet. Gravity can be an important driving term, especially for refrigerated and semi-refrigerated NH_3.

It has been assumed in deriving Equation (1) that the flow is homogeneous (i.e. there is no slip between the two phases), frictionless, and adiabatic (i.e. there is no heat transfer through the pipe walls) and that no work is done on the surroundings (i.e. the pipe and tank do not move). Because of these assumptions, there is no change in entropy between the inlet and outlet.

The discharge rate, G, in terms of V_4 is given by

$$G = \frac{V_4 A_4}{v_4} \qquad \ldots (2)$$

where A_4 is the cross-sectional area of the outlet and v_4 is the specific volume of the fluid at the outlet.

2.2.1 *Liquid discharge*

For liquid discharge compressibility can be neglected and Equation (1) simplifies to

$$\tfrac{1}{2} V_4^2 = \alpha_P^2 \left[(P_2 - P_4)/\rho_L + gh\right] \quad \ldots (3)$$

where ρ_L is the liquid density.

2.2.2 *Equilibrium two-phase discharge*

For equilibrium flow, an expression is required for the dependence of v on P in order to do the integration in Equation (1). This can be found by exploiting the assumption that entropy is conserved along the flow path. The entropy is the sum of contributions from the liquid and vapour which when equated to the initial fluid entropy results in

$$C_L \ln T_2 = C_L \ln T + \frac{Q\Delta h\,(T)}{T} \quad \ldots (4)$$

(Hall[14]), where

C_L is the specific heat of the liquid (assumed constant)

T_2 is the fluid temperature at the inlet

T is the fluid temperature at any point along the flow path

Q is the quality at that point (the mass fraction of vapour, and

$\Delta h\,(T)$ is the heat of vaporisation per unit mass at the temperature T.

The specific volume in terms of Q is

$$v = v_L + Q\,(v_V - v_L) \quad \ldots (5)$$

where v_L and v_V are the specific volumes of liquid and vapour respectively. Substituting for Q results in

$$v = v_L + \frac{(v_V - v_L)\,T\,C_L \ln (T_2/T)}{\Delta h\,(T)}. \quad \ldots (6)$$

A convenient way to specify $\Delta h\,(T)$ is to use the Clausius-Clapeyron equation, which gives

$$\Delta h\,(T) = T\,(v_V - v_L)\,\frac{dP^0}{dT}. \quad \ldots (7)$$

The integral in Equation (1) can now be done with the result

$$\tfrac{1}{2} V_4^2 = \alpha_P^2 \left[(P_2 - P_4)/\rho_L + C_L\,(T_2 - T_4) - C_L\,T_4 \ln (T_2/T_4) + gh\right] \quad \ldots (8)$$

Note that P_4 is the major independent variable with T_4 given by the condition of vapour-liquid equilibrium.

2.2.3 *Non-choked flow*

In non-choked flow P_4 is ambient pressure and Equation (8) with Equations (2), (4) and (6) are sufficient to determine G; dP^0/dT is evaluated from the saturated vapour pressure equation which is taken to be

$$P^0 = e^{-A^0/T + B^0} \qquad \ldots (9)$$

which gives

$$\frac{dP^0}{dT} = \frac{P^0 A^0}{T^2}. \qquad \ldots (10)$$

The specific volume at the outlet then becomes

$$v_4 = v_L + \frac{C_L T_4^2}{P_4 A^0} \ln (T_2/T_4) \qquad \ldots (11)$$

2.2.4 *Choked flow*

The condition for choked flow is that the flow rate should be a maximum for variations in the outlet pressure. This condition implies the flow speed cannot exceed the speed of sound in the equilibrium mixture. (It is assumed that choking occurs at the outlet. This will not be so if the cross-sectional area of the pipe is less upstream in which case the minimum area should be used in the formulae to be derived.) This is most conveniently expressed as

$$\frac{dG^2}{dP_4} = 0. \qquad \ldots (12)$$

From Equations (1) and (2) this gives

$$\left(\int_{P_4}^{P_2} v \, dP + gh\right) \left.\frac{dv}{dP}\right|_4 + \tfrac{1}{2} v_4^2 = 0. \qquad \ldots (13)$$

$dv/dP|_4$ is found straightforwardly from Equation (11). The complete equation which determines the choking pressure is

$$\left\{v_L (P_2 - P_4) + C_L (T_2 - T_4) - C_L T_4 \ln (T_2/T_4) + gh\right\} \frac{C_L T_4^3}{P_4^2 A^{02}}$$

$$\times \left\{1 + \left(\frac{A^0}{T_4} - 2\right) \ln (T_2/T_4)\right\} = \tfrac{1}{2} \left\{v_L + \frac{C_L T_4^2}{P_4 A^0} \ln (T_2/T_4)\right\}^2 \qquad \ldots (14)$$

This transcendental equation can be solved numerically with T_4 as the unknown. The flow will be choked if $P_4 = P^0 (T_4)$ exceeds atmospheric pressure.

2.2.5 *The outlet quality*

Whether the flow is choked or not, the quality of the flow at the outlet is given by

$$Q_4 = \frac{C_L T_4^2}{A^0 P_4} \frac{\ln (T_2/T_4)}{(v_{V4} - v_L)}. \qquad \ldots (15)$$

where v_{V4} is the specific volume of the vapour at the outlet and is evaluated from the perfect gas law

$$P_4 v_{V4} = \frac{R T_4}{W}. \qquad \ldots (16)$$

R is the universal gas constant and W is the molecular weight of NH_3.

It may be necessary to include friction in this analysis for flows via long pipes. This would entail solving an ordinary differential equation when the hydrostatic term is included and is beyond the scope of the present study.

3. FLASHING AT THE OUTLET

The equations presented in Section 2 provide estimates for properties of the flow at the outlet. The fluid at the outlet may be superheated for two reasons:

(i) The flow is liquid in the pipe

Here the outlet pressure is atmospheric but the temperature of the liquid is the original temperature in the tank and so unless the liquid in the tank was fully refrigerated the liquid will flash.

(ii) The flow is two-phase in the pipe and choked at the outlet

Here the outlet pressure is greater than atmospheric and so the mixture will flash when the pressure decreases to ambient downstream of the outlet. This instance is sometimes called an under-expanded two-phase jet. (Flashing will not occur at the outlet if the flow is choked upstream; the formulae for flow downstream of the choke are not given but are straightforward to derive.)

Next, equations are derived for the evolution of the flow from the outlet to a point where the pressure becomes atmospheric and the fluid is in equilibrium, for both the cases above. First, a few general remarks are made.

Very little is known either experimentally or theoretically about the behaviour of superheated two-phase jets. Considerable work has been done, however, on underexpanded gaseous jets, as reviewed by Ramskill.[32] Depressurisation causes rarefraction waves and shocks near the outlet in such jets, and the complexity of the pattern of waves and shocks increases markedly with increasing overpressure at the outlet. A consequence of the presence of the shocks is that neither enthalpy nor entropy are conserved in the flow.

The thermodynamic behaviour of a two-phase jet at the outlet is important for determining the eventual flash fraction. It is commonly assumed that enthalpy is conserved during depressurisation to ambient pressure in order to estimate this flash fraction. We will see that this is not strictly valid and that an estimate is required for the change in enthalpy of the flashing jet in order to obtain a proper estimate of the flash fraction.

Detailed modelling of two-phase flashing jets is beyond the scope of the present work and in any case would not be justified in view of the paucity of experimental data. Modelling the transient behaviour of the flow is therefore not done. However, information can be obtained from a consideration of conservation of mass, momentum and energy. It will be seen below that certain assumptions are made about the nature of the flow in order to close the equations. Specifically, no entrainment of air and no loss of momentum or heat to the air surrounding the jet is assumed. All the assumptions can only be justified **a posteriori** either by comparison with data, of which none suitable exists at present, or with a more thorough treatment. These options are left for future studies.

There are essentially three quantities which define the flow field. These are the cross-sectional area of the jet, A, the average axial velocity, V, and the specific volume, v. We wish to relate values of these quantities after flashing to those at the outlet.

It is assumed that the jet has half-angle θ after flashing and that the flow is radial and independent of direction. Conservation equations are obtained by integration over a surface, S, composed of elements S_4, S_{45} and S_5. A schematic diagram is shown in Fig. 2; S_4 is the exit plane of the pipe with area A_4; S_5 is a spherical cap with area A_c over which the pressure is atmospheric and the two phases are in thermal equilibrium; S_{45} is the surface of the jet between S_4 and S_5 defined such that the flow is parallel to the surface and at atmospheric pressure.

Assuming that no air is entrained into the jet, conservation of mass flux requires that:

$$G = \frac{V_4 A_4}{\nu_4} = \frac{V_c A_c}{\nu_c} \quad \ldots (17)$$

where subscript c denotes conditions on S_5 and V_c is the flow speed normal to S_5.

An equation for conservation of momentum is obtained from the momentum flux tensor (Landau and Lifschitz[20]), taken as

$$\Pi_{ij} = P \delta_{ij} + \frac{1}{\nu} V_i V_j, \qquad i,j = 1,3, \quad \ldots (18)$$

where P is pressure, δ_{ij} is the Kronecker delta function, V_i is the mean velocity field, ν is the specific volume and viscous and turbulent stress terms have been neglected. Integrating this over the surface S and assuming steady state and projecting the result onto the jet axis, $\underline{n}$, results in

$$\int_S P (d\underline{S} \cdot \underline{n}) + \int_S \frac{1}{\nu} (\underline{V} \cdot \underline{n}) (\underline{V} \cdot d\underline{S}) = 0. \quad \ldots (19)$$

Doing the integrals results in the equation

$$- A_4 (P_4 - P_a) - \frac{1}{\nu_4} V_4^2 A_4 + \frac{1}{\lambda \nu_c} V_c^2 A_c = 0 \quad \ldots (20)$$

where A_c/λ is the area of S_5 seen end-on; λ is given by

$$\lambda = \frac{2}{1 + \cos\theta}. \quad \ldots (21)$$

This can be simplified by using the mass-flux equation, Equation (17), to obtain

$$V_c/\lambda = V_4 + (P_4 - P_a) A_4/G. \quad \ldots (22)$$

Conservation of energy is expressed by Bernoulli's theorem (Batchelor[2]) in the form

$$U_4 + P_4 \nu_4 + \tfrac{1}{2} V_4^2 = U_c + P_a \nu_c + \tfrac{1}{2} V_c^2. \quad \ldots (23)$$

U_4 and U_c are the specific internal energies of the flow at the outlet and after flashing respectively.

It can be seen from Equation (23) that enthalpy is not conserved during flashing – the change in enthalpy is in general negative due to acceleration of the flow. The second law of thermodynamics requires that the change in entropy is zero or positive – in this case it will in general be positive because the expansion is non-reversible. This can be used to obtain a lower bound on the change in enthalpy if desired.

An expression is required for U at S_4 and S_5 where the liquid at S_4 may be superheated even though it is at the same temperature as the vapour.

The total specific internal energy, U, is

$$U = (1 - Q) C_L T + Q U_V \quad \ldots (24)$$

where

Q is the mass fraction of vapour in the flow

C_L is the liquid specific heat, and

U_V is the vapour specific internal energy.

The thermodynamic path chosen to evaluate U_V is a path of constant temperature starting with superheated liquid at pressure P and temperature T. The liquid vaporises at the saturated vapour pressure $P^0(T)$ and then returns to P and T as vapour. The result for U_V is

$$U_V = C_L T + \Delta h(T) - (\nu_V - \nu_L) P^0(T) + \int_{P^0(T)}^{P} dU. \quad \ldots (25)$$

The last term is the change in internal energy of the vapour along the path of constant temperature. This is zero for an ideal gas and so U becomes

$$U = C_L T + Q \{\Delta h(T) - (\nu_V - \nu_L) P^0(T)\} \quad \ldots (26)$$

Q is known at the outlet from the pipe and so only $\Delta h(T)$ remains to be determined to find U_4. Equations (7) and (10) are used, resulting in

$$U_4 = C_L T_4 + Q_4 (\nu_{V4} - \nu_L) P_4 \left(\frac{A^0}{T_4} - 1\right) \quad \ldots (27)$$

To evaluate U_c one uses Equations (5), (7) and (10) to eliminate Q and Δh from Equation (26) obtaining

$$U_c = C_L T_c + (\nu_c - \nu_L) P_a \left(\frac{A^0}{T_c} - 1\right) \quad \ldots (28)$$

Collecting the results in Equations (23), (27) and (28) finally gives

$$C_L T_4 + P_4 \nu_4 + Q_4 P_4 (\nu_{V4} - \nu_L) \left(\frac{A^0}{T_4} - 1\right) + \tfrac{1}{2} V_4^2$$

$$= C_L T_c - P_a \nu_L \left(\frac{A^0}{T_c} - 1\right) + \tfrac{1}{2} V_c^2 + P_a \nu_c \frac{A^0}{T_c} \quad \ldots (29)$$

V_c can be found from the momentum equation given earlier and so the energy equation is used to find ν_c. This in turn enables Q_c to be found from Equation (5) and A_c is found from the mass equation.

Downstream conditions are taken to be constant on a plane perpendicular to the jet axis with flow parallel to the axis. It is therefore necessary to translate the quantities (A_c, V_c, ν_c, U_c and T_c) specified on the spherical cap, to an equivalent set of quantities (A_5, V_5, ν_5, U_5 and T_5) specified on a plane normal to the axis. The composition of the two-phase mixture is taken to be unchanged and so $\nu_5 = \nu_c$, $U_5 = U_c$ and $T_5 = T_c$. A_5 and V_5 are chosen to conserve mass and momentum with the results

$$V_5 = V_c/\lambda \quad \ldots (30)$$

and

$$A_5 = \lambda A_c. \quad \ldots (31)$$

Note that V_5 is the mean axial flow speed.

4. MAXIMUM DROP SIZE AND IMPLICATIONS FOR RAIN-OUT

There are two reasons for considering fragmentation of the liquid part of the jet and the possibility of rain-out of the resulting drops. Firstly, loss of liquid can have a substantial effect on the mass flux of NH_3 in the jet. If the NH_3 is pressurised or semi-refrigerated then the flash fraction is typically 20% or 10%. If all the residual liquid rained out then the mass flux of NH_3 would decrease

by a factor of 5 or 10. If the NH_3 is refrigerated then there may be no residual jet after rain-out. Secondly, the presence of suspended liquid in the jet will have a large effect on the density, primarily through cooling by evaporation. The density in turn is known to have an important effect on the rate of dilution of the jet.

It is assumed in what follows that the liquid or two-phase jet is horizontal and that it does not impinge onto a solid surface. The experiments reviewed in Part I suggest that impingement causes extra liquid to be removed from the jet. It is therefore conservative to ignore this.

A criterion for assessing whether rain-out can be ignored is developed by first estimating the largest stable drop size downstream of the outlet and then comparing the gravitational settling velocity of these drops with their horizontal velocity in the jet. If this results in a trajectory close to the jet axis, compared to the divergence angle of the jet due to air entrainment, then it is argued that rain-out can be ignored. A horizontal jet, which we treat here, is the simplest case because the gravitational motion of the drops is decoupled from their motion along the jet axis. Other jet attitudes require a more complex treatment.

4.1 Liquid fragmentation

Fragmentation of the liquid is caused by fluid instability and by flashing. Low-speed liquid jets are unstable and break up into drops of size comparable to the jet diameter. At higher speeds large drops are unstable because of surface stresses due to their motion and so the jet becomes atomised. If the fluid is superheated then drops are also formed by bursting of bubbles within the liquid.

Once drops are formed they may be small enough to remain suspended until completely vaporised. Larger drops are affected by gravity and they may settle out before they have completely evaporated. Their velocities differ from that of the surrounding air and vapour, and vaporisation is primarily caused by entrainment of air into the turbulent wake of each drop. A jet with differing drop and vapour velocities is said to be non-homogeneous. Homogeneous jets, in which the drops are smaller and there is no velocity difference, are discussed in Section 5.

Detailed modelling of the processes discussed above is not done here. A simplified treatment is offered aimed at establishing whether or not rain-out is likely to be important. An estimate of the maximum initial drop size is used to estimate the initial trajectory of the drops and so determine whether rain-out is important. The results will not apply when the jet impinges on a solid surface.

Break-up due to flashing is considered first. Very little is known about this. Brown and York (1962) studied low-speed, slightly superheated jets of water experimentally. They show that there is a minimum superheat required for break-up, if the jet speed is low enough for it to be stable mechanically. They find a correlation for this minimum superheat by showing that the critical jet Weber number for fragmentation depends on the bubble growth-rate constant. They also show that the mean drop diameter times the jet Weber number is reasonably correlated with the bubble growth-rate constant. Although these experiments provide valuable information on this mode of break-up, the correlations are valid only for water; it is not clear how they should be non-dimensionalised to apply them to other substances.

Koestel, Gido and Lamkin[18] theoretically estimated drop sizes for loss-of-coolant accidents in pressurised water reactors. They assume that flashing bubbles form in the water and grow to a size determined from Brown and York's results for the bubble growth rate constant at fragmentation. The bubbles then burst and form drops of a size calculated by assuming conservation of surface energy. Again, it is not known how to extrapolate to different liquids. Also, the assumption that surface energy is conserved was not verified experimentally and not justified theoretically.

Thus drop size after flashing cannot readily be estimated. However, when the NH_3 is either semi-refrigerated or pressurised, the discharge speed is large because of the high driving pressure. This results in small drops by mechanical break-up. It is shown in Wheatley[40] that the drop size so obtained is sufficient to explain the lack of rain-out in these cases. So break-up by flashing is not considered further here.

Of greater interest are refrigerated releases, when only mechanical break-up can occur. Driving pressures are much less than for superheated releases even for hydrostatic heads up to 25 m or so, and so drops are larger. No experimental results are available for refrigerated releases but there is some evidence from an accident at Blair in the USA, reported by MacArthur,[22] that significant vaporisation is possible before the liquid settles on the ground.

Brodkey[5] describes the behaviour of an unsaturated liquid jet. At low speeds the jet breaks up to form large drops. The maximum drop size, d_D, can be estimated from

$$d_D = 1 \cdot 89\ d_5\ (1 + 3\ We_J^{½}/Re_J)^{½} \qquad \ldots (32)$$

where d_5 is the diameter of the jet before break-up, Re is the jet Reynolds number given by

$$Re_J = \frac{V_5\ d_5\ \rho_L}{\mu_L} \qquad \ldots (33)$$

with μ_L the liquid viscosity. We_J is the jet Weber number given by

$$We_J = \frac{V_5^2\ d_5\ \rho_L}{\sigma_L} \qquad \ldots (34)$$

σ_L is the coefficient of surface tension. The first term inside the brackets in Equation (32) stems from Rayleigh's[33] theory of break-up of liquid columns and the second term is a viscous correction due to Weber.[39]

As the jet speed increases, the connected portion increases in length and decreases again, passing through regimes of varicose and sinuous instability, according to Brodkey, until the jet atomises at the outlet at a critical speed. Ohnesorge[28] found experimentally that atomisation occurs when

$$We_J \geqslant Re_J^{-0.45} \times 10^6. \qquad \ldots (35)$$

Drops will be smaller than given by Equation (32) when the jet is sinuous or atomised. Large drops are unstable because of aerodynamic stresses at the surface of the drop which overcome the restoring effect of surface tension. The maximum stable drop size found from experiment, according to Brodkey, is given by

$$We_D = \frac{V_5^2\ d_D\ \rho_a}{\sigma_L} = 20. \qquad \ldots (36)$$

We_D is the drop Weber number at the outlet with ρ_a the density of air.

In principle V_c should be used here in place of V_5 but has been omitted because of uncertainty in the value of λ.

For further analysis the maximum drop size is taken to be the minimum of the values from Equations (32) and (36).

4.2 The gravitational settling velocity of drops

The maximum stable drop size d_D can be used to estimate the maximum speed at which drops descend from the jet. This is taken to be the terminal gravitational settling speed, V_D, and is found by balancing the drag force against gravity resulting in the following implicit equation for the Reynolds number, Re_D.

$$\eta\ Re_D^2\ C_D\ (Re_D) = \frac{4}{3}\ d_D^3\ \frac{(\rho_L - \rho_a)\ \rho_a\ g}{\mu_a^2} \qquad \ldots (37)$$

where

$$Re_D = \frac{V_D\, d_D\, \rho_a}{\mu_a}. \qquad \ldots (38)$$

C_D is the drag coefficient for a rigid spherical drop and η is a correction factor for the motion of fluid within the drop, given by

$$\eta = \frac{1 + \mu_a/\mu_L}{1 + \frac{2}{3}\,\mu_a/\mu_L} \qquad \ldots (39)$$

(Batchelor[2]) where μ_a is the viscosity of air.

The drag coefficient is expressed as

$$C_D = \frac{24}{Re_D} + C'_D \qquad \ldots (40)$$

The first term is Stokes law, valid for $Re_D \lesssim 1$, and C'_D is a correction which accounts for inertia and turbulence effects not included in Stokes law. In our calculations C'_D is obtained as a piecewise linear fit to experimental measurements of the residue $C_D - 24/Re_D$ given by Batchelor,[2] as a function of $\log_{10} Re_D$ for $1 \leqslant Re_D \leqslant 10^{6.5}$; C'_D was evaluated twice per decade.

The result for the terminal gravitational settling velocity is shown in Fig. 3 as a function of the drop diameter. Drops have to have diameters $\gtrsim 0 \cdot 3$ mm before the settling velocity exceeds $\sim 1\ ms^{-1}$.

In this calculation, the drop is assumed to remain spherical. This will be so if surface tension is large enough to resist the stresses on the drop due to its motion. It is easily verified that this will always be so for $Re_D \lesssim 1$. For larger Reynolds numbers we require

$$We_D = \frac{V_D^2\, d_D\, \rho_a}{\sigma_L} \ll 1. \qquad \ldots (41)$$

It is assumed here that the drop has horizontal speed equal to the jet speed. The drop therefore moves with speed V_D with respect to the surrounding fluid. However, we know from the criterion determining the maximum size of the drop at the outlet that

$$d_D \leqslant \frac{20\,\sigma_L}{V_5^2\,\rho_a} \qquad \ldots (42)$$

and so we require

$$\frac{V_D^2}{V_5^2} \ll \frac{1}{20} \qquad \ldots (43)$$

We shall see below that our criterion for drops to remain in the jet requires that $V_D \leqslant V_5/10$, and so Equation (41) is satisfied in such a way as to ensure the valid application of the rain-out criterion.

4.3 The criterion for rain-out

The mean initial trajectory of the largest stable drops is at an angle φ to the horizontal roughly given by

$$\tan\varphi = \frac{V_D}{V_s} \quad \ldots (44)$$

Smaller drops will have trajectories closer to the jet axis. It is assumed that rain-out is not significant if

$$\varphi \leqslant \beta \quad \ldots (45)$$

where β is the half-angle of divergence of the homogeneous momentum jet (see Section 5 below). β is given by Equation (55).

Combining the estimates for drop size and settling speed leads to a dependence of the terminal gravitational settling speed of the largest stable drop on the axial speed of the jet at the outlet as shown in Fig. 4. The criterion for rain-out corresponds to the region above a line of slope 1 on the log-log plot. The position of the line depends on the composition at the outlet and is illustrated for a liquid jet in Fig. 4.2. Here, rain-out is unlikely to be important if the axial speed is less than about 30 ms^{-1}. The critical axial jet speed is smaller than this for two-phase jets.

When rain-out occurs, the parameters of the residual jet need to be specified. It is assumed the momentum of the vapour fraction is unaffected and so the jet speed is unchanged. The cross-sectional area of the jet will be slightly decreased by the reduction in mass flux of NH_3.

5. ENTRAINMENT OF AIR

When the aerosol particles are small enough, motion in the jet will be homogeneous. The jet will entrain air through shear-flow turbulence and so will broaden and slow down. The rate at which air is entrained determines the length of the jet. Thermodynamic properties are determined directly from the amount of air in the jet. These two aspects are dealt with in the succeeding sub-sections.

5.1 The homogeneous momentum jet

Equations which describe the behaviour of a steady homogeneous momentum jet can be written as follows (see e.g. Turner[38]) where we assume the lateral profiles have a 'top-hat' form and that the diffusivities of matter and momentum are equal. The mass flux of NH_3 is conserved and so

$$G_6 = A\,V\,C \quad \ldots (46)$$

where

G_6 is the mass flux after rain-out and before air entrainment;

A is the cross-sectional area of the jet;

V is the speed of the jet; and

C is the NH_3 mass concentration including both vapour and aerosol.

The axial momentum flux integrated across the jet is also conserved and so

$$G_6 V_6 = A\,V^2\,\rho \quad \ldots (47)$$

where

V_6 is the speed of the jet before air entrainment; and

ρ is the density of the jet.

This equation can be written in terms of the mass flux of air in the jet, G_a, as

$$G_6 V_6 = V (G_6 + G_a) = VG \quad \ldots (48)$$

Atmospheric turbulence is assumed to take over from the jet-flow turbulence as the dominant cause of dilution when

$$V = U_W \quad \ldots (49)$$

(Cude[8]). Here U_W is the wind speed at the height of the jet axis. This criterion will be valid only if gravity effects do not become important prior to Equation (49) being satisfied. This is discussed further by Wheatley.[40]

Equations (46), (47) and (49) are sufficient to determine starting conditions for subsequent atmospheric dispersion calculations. To find the length of the jet, and thus the point at which to apply these conditions, one must also specify the entrainment rate.

For a fully turbulent jet, dimensional reasoning gives the relation

$$\frac{d G_a}{dz} = 2\pi R V \rho_a f (\rho/\rho_a) \quad \ldots (50)$$

where

z is the distance downstream from the outlet

R is the jet radius

ρ_a is the ambient air density; and

f is a function of ρ/ρ_a, as yet unspecified.

Turner[38] has reviewed experiments of entrainment into turbulent momentum jets. Ricou and Spalding[36] used a particularly accurate method for measuring the axial mass flow rate in the jet. For isothermal jets over a range of initial densities, they concluded that entrainment was accurately described by

$$\frac{d G_a}{dz} = \pi^{1/2} . \tan \beta_\infty \rho_a^{1/2} V^{1/2} G^{1/2} \quad \ldots (51)$$

where $\tan \beta_\infty$ is a constant equal to $0 \cdot 159$ (β_∞ is the asymptotic half-angle of the jet, equal to $9 \cdot 1^0$. $\frac{1}{2} \tan \beta_\infty$ is sometimes called the entrainment coefficient). Equations (50) and (51) imply

$$f (\rho/\rho_a) = \tfrac{1}{2} \tan \beta_\infty (\rho/\rho_a)^{1/2} . \quad \ldots (52)$$

This suggests density affects entrainment close to the start of an NH_3 jet where ρ usually deviates significantly from ρ_a. This can be seen explicitly for an isothermal gas jet whose half-angle is found to obey

$$\tan \beta = \tfrac{1}{2} (\rho_a/\rho + 1) (\rho/\rho_a)^{1/2} \tan \beta_\infty \quad \ldots (53)$$

As ρ tends to ρ_a, β approaches β_∞ from above. A similar result is obtained for non-isothermal two-phase jets but cannot be expressed in a simple analytic form.

This conflicts with the experimental observation reviewed in Part I which suggest that β is smaller than β_∞ by a factor of ~ 2. Also, Yoshinobu and Saima[44] have studied gaseous isothermal jets close to the orifice and conclude that β is smaller than β_∞ when ρ is greater than ρ_a. The root of this conflict lies in Equation (51) which was verified by Spalding and Ricou for $z/R (0) \geqslant 40$ for which ρ was at most about $1 \cdot 05 \rho_a$ in their experiments. It is therefore concluded that this equation is not valid when ρ differs significantly from ρ_a.

Morton, Taylor and Turner[25] suggest that f is independent of ρ/ρ_a. This is supported indirectly by experimental evidence of entrainment into gaseous gravity currents which shows that the entrainment rate is independent of ρ/ρ_a.[42] If f is assumed constant,

$$f\,(\rho/\rho_a) \;=\; \tfrac{1}{2}\,\tan\beta_\infty, \qquad \ldots (54)$$

then we readily find for a gaseous isothermal jet that

$$\tan\beta \;=\; \tfrac{1}{2}\,(\rho_a/\rho + 1)\,\tan\beta_\infty \qquad \ldots (55)$$

from which it is clear than β is less than β_∞ when ρ is greater than ρ_a. Numerical calculations for discharge of pressurised NH_3 via a 10 metre pipe into air at 20°C and 80% relative humidity give $\beta \sim 5°$ close to the orifice, in agreement with the experimental observations. This supports the use of Morton et al's entrainment assumption rather than Ricou and Spalding's.

Morton et al's entrainment equation cannot be integrated analytically in terms of z even for the case of an isothermal gaseous jet; however Ricou and Spalding's equation can be integrated to give a useful scaling law valid where the jet density is close to that of air. The result is

$$\frac{G_6}{G_a} \;=\; \frac{C}{\rho - C} \;=\; \frac{L}{z} \qquad \ldots (56)$$

where L is a length scale defined by

$$L \;=\; G_6^{1/2}/V_6^{1/2}\,\pi^{1/2}\,\rho_a^{1/2}\,\tan\beta_\infty$$

$$\;=\; R_6\,\rho_6^{1/2}/\rho_a^{1/2}\,\tan\beta_\infty. \qquad \ldots (57)$$

For $z/L \gg 1$, $C \ll \rho$ so that $\rho \approx \rho_a$ justifying use of Equation (52). We then find that C is proportional to $G_6^{1/2}/V_6^{1/2}$ (or equivalently $R_6\,\rho_6^{1/2}$) at any given distance z.

5.2 The thermodynamics of mixing ammonia with moist air

Mixing of moist air into the jet is assumed to occur adiabatically and isobarically and so enthalpy is conserved. This enables the thermodynamic state of the mixture to be found in terms of the ratio of the masses of air and NH_3. The method used to find the thermodynamic state of the mixture is outlined here.

Essentially six quantities characterise the mixture state. These are: temperature; the volume occupied by the vapour phase; the quantity of liquid present and its composition; and the partial pressures of NH_3 and H_2O vapour. The equations which determine these quantities are: conservation of enthalpy (because the process takes place at constant pressure); the equations of state for dry air, NH_3 vapour and H_2O vapour; and the equilibrium partial pressures of NH_3 and H_2O above the liquid mixture. The formula for the change in enthalpy, ΔH, incurred when NH_3 and moist air are mixed together and brought to some final arbitrary temperature is given in Appendix 1. The vapour phases are assumed to behave as perfect gases. Formulae for the equilibrium partial pressure of NH_3 and H_2O are given in Appendix 2.

These equations do not admit any simple method of solution. The final temperature of the mixture in particular cannot be eliminated from the equations in any simple way. It is most convenient to find it implicitly from the equation

$$\Delta H\,(T) \;=\; 0 \qquad \ldots (58)$$

by an iterative numerical method.

It is necessary to know whether liquid is present before ΔH can be found for any estimated value for T. This is done by first assuming that a liquid phase does not exist and testing to see if the resulting vapour phase (for which the equations are easy to solve) is super-saturated. The details are given in Appendix 3.

If it has been established that a liquid phase exists for some value of T then the equations which determine the equilibrium state of the mixture are still not easy to solve, essentially because the liquid phase composition, denoted here by X – the molar fraction of NH_3 in the liquid mixture – couples the equations for the equilibrium partial pressures and the equations of state for the vapour phases. An implicit equation is found for X and solved iteratively. The range of search for X has to be restricted to ensure that the solution found is physical. The details are described in Appendix 4.

6. CONCLUSIONS

A model for discharge of liquefied NH_3 into moist atmospheres has been developed using the results of the survey of experimental data done in Part I.

The main ingredients of the model are:

- either liquid or homogeneous equilibrium two-phase flow to the outlet;
- choking at the outlet;
- a treatment for flashing at the outlet;
- a criterion for whether rain-out is likely to be important; and
- entrainment of moist air into a homogeneous two-phase momentum jet.

The model enables initial conditions for subsequent atmospheric dispersion calculations to be estimated. It is applicable to a wide range of storage conditions of NH_3 including refrigerated, semi-refrigerated and pressurised storage of liquefied NH_3.

Lastly, the model could be used for other hazardous chemicals, such as chlorine and hydrogen fluoride, with changes of physical constants.

7. APPENDIX 1

The change in enthalpy when ammonia and moist air are mixed together

An equation is required for the total change in enthalpy when a mixture of NH_3 liquid and vapour at some initial temperature T_i are mixed with moist air at ambient temperature T_a to form an equilibrium mixture at a final temperature, T, where the final state may consist of a binary liquid phase in addition to a vapour phase.

The thermodynamic paths chosen to evaluate the change in enthalpy are shown in Fig. A1.1. The paths for vaporisation are chosen so that heats of vaporisation are required only at a single reference temperature, T_r. The total change in enthalpy is the sum of contributions as follows:

$$\Delta H = \Delta H_1 + \Delta H_2 + \Delta H_3 + \Delta H_{12}. \qquad \ldots (A1.1)$$

Subscripts 1, 2, 3 and 12 stand for water, NH_3, dry air and the binary liquid mixture.

The contribution for water is

$$\Delta H_1 = \{N_{1L}\, C_{L1}\, (T - T_r) - N_{1L}\, \Delta h_1\, (T_r) + N_1\, C_{V1}\, (T_r - T_a) + (N_1 - N_{1L})\, C_{V1}\, (T - T_r)\}\, W_1 \qquad \ldots (A1.2)$$

where N_1 is the total number of moles of water present, N_{1L} is the number of moles of liquid water formed during mixing, C_{L1} and C_{V1} are the specific heats at constant pressure of water liquid and vapour respectively, W_1 is the molecular weight of water and $\Delta h_1\ (T_r)$ is the heat of vaporisation of water evaluated at the reference temperature T_r.

The contribution for NH_3 is

$$\Delta H_2 = \{Q\, N_2\, C_{V2}\, (T_r - T_i) + (N_2 - N_{2L})\, C_{V2}\, (T - T_r) + [(1 - Q)\, N_2 - N_{2L}]\, \Delta h_2\, (T_r) + (1 - Q)\, N_2\, C_{L2}\, (T_r - T_i) + N_{2L}\, C_{L2}\, (T - T_r)\}\, W_2 \qquad \ldots (A1.3)$$

Q is the mass fraction of vapour in the initial two-phase NH_3 mixture and all the other quantities are defined similarly to those for water.

The contribution for dry air is

$$\Delta H_3 = N_3\, C_{V3}\, (T - T_a)\, W_3 \qquad \ldots (A1.4)$$

The change in enthalpy in forming the binary liquid mixture is found from Wheatley[41] as

$$\Delta H_{12} = -\,(N_{1L} + N_{2L})\, (1 + r_A - \tfrac{1}{2}\, r_A\, X)\, X\, (1 - X)\, R\, w_A. \qquad \ldots (A1.5)$$

r_A and w_A are the constants in the expressions for the saturated vapour pressures of NH_3 and water above the liquid mixture, R is the universal gas constant and X is given by

$$X = \frac{N_{2L}}{N_{1L} + N_{2L}}. \qquad \ldots (A1.6)$$

The specific heats have all been assumed to be independent of temperature. In all practical cases this is a reasonable approximation since the temperature range over which this is assumed is small compared to the critical temperatures of water, NH_3 and air.

8. APPENDIX 2

Saturated vapour pressures of ammonia and H_2O above liquid mixtures

The formalism of Wheatley[41] is used to express the saturated vapour pressures of NH_3 and H_2O above liquid mixtures in a form convenient for the calculations required by the model. Details of how the parameters in the saturated vapour pressure formulae are determined are given and the effect of uncertainty in the parameters on predictions of the model is assessed.

Wheatley's formulae are

$$P_1^s(T, X) = (1 - X)\, P_1^0 \exp(-A_1/T + B_1) \quad \ldots (A2.1)$$

and

$$P_2^s(T, X) = X\, P_2^0 \exp(-A_2/T + B_2) \quad \ldots (A2.2)$$

where P_1^s and P_2^s are the saturated vapour pressures of H_2O and NH_3 respectively in equilibrium above a liquid mixture with molar fraction of NH_3 equal to X. T is the absolute temperature. P_1^0 and P_2^0 are the saturated vapour pressures of the pure substances, approximated here by

$$P_1^0 = \exp(-A_1^0/T + B_1^0) \quad \ldots (A2.3)$$

and

$$P_2^0 = \exp(-A_2^0/T + B_2^0) \quad \ldots (A2.4)$$

where A_1^0, A_2^0, B_1^0 and B_2^0 are constants. A_1, A_2, B_1, B_2 are functions of X given by

$$A_1 = (a + \tfrac{3}{2} r_A - r_A X)\, X^2 w_A \quad \ldots (A2.5)$$

$$A_2 = (1 + r_A - r_A X)\, (1 - X)^2 w_A \quad \ldots (A2.6)$$

$$B_1 = (1 + \tfrac{3}{2} r_B - r_B X)\, X^2 w_B \quad \ldots (A2.7)$$

$$B_2 = (1 + r_B - r_B X)\, (1 - X)^2 w_B \quad \ldots (A2.8)$$

Values of saturated vapour pressure for the NH_3 - H_2O system are given by Macriss et al.[23] These values were obtained by correlating the data of Scatchard[37] and Pierre[31] on a Cox-Othmer plot. The data of Scatchard were in turn obtained from a correlation of the data of Perman[29] and Wucherer.[43] Only the data of Wucherer apply for $X \geqslant 0{\cdot}4$, since Macriss et al[23] show that Scatchard's values do not correlate well with Wucherer's for X in this range. Macriss et al give saturated vapour pressures for temperatures down to $-50°C$ although data were available only for T greater than 0°C.

Macriss et al's results for $0 \leqslant X \leqslant 1$ and $-50°C \leqslant T \leqslant 40°C$ are used here. Values of A_1^0, $A^0{}_2$, B_1^0, B_2^0, A_1, A_2, B_1 and B_2 were found by choosing fixed values for X and then doing linear regressions of log P_1^s and log P_2^s against 1/T.

A_1^0, A_2^0, B_1^0 and B_2^0 were accurately determined; the correlation coefficient was in each case better than 0·99999.

A_1, A_2, B_1 and B_2 were less accurately determined. The resulting values are plotted in Figs 5 and 6. The correlation was found to be slightly improved when the range of T was restricted to 5 - 40°C. The results for this restricted range of T are also shown in the figures.

A comparison of the values found for A_1, A_2, B_1 and B_2 with the results of Wheatley[41] shows that the data are inconsistent. A possible explanation for this is the discrepancy between those recommended by Scatchard, incorporated in the values recommended by Macriss et al, and the data of Wucherer. This is corroborated by a comparison between the heat of mixing found from A_1 and A_2 and direct measurements by Zinner in 1934 given by Macriss et al and shown in Fig. 8. Good

agreement is obtained for $X \leqslant 0 \cdot 4$ but the agreement is poor for larger values of X. Greater emphasis has therefore been given to the data for $X \leqslant 0 \cdot 4$ when fitting the formulae (A2.5) - (A2.8).

There is a clear asymmetry between A_1 and A_2 and between B_1 and B_2. The closest match to this asymmetry is given by $r_A = r_B = -14$. This results in a minimum in the heat of mixing at $X = 0 \cdot 41$ which agrees fairly well with direct measurements. By matching the data in the range $X \leqslant 0 \cdot 4$ it was found that $w_A = -185$ and $w_B = -0 \cdot 34$.

The resulting correlations for A_1, A_2, B_1 and B_2 are shown in Figs 9 and 10 together with the data for the reduced range of T. The correlation for the heat of mixing is shown in Fig. 11. Close agreement is obtained between the data and correlations except for A_1 and B_1 and the heat of mixing for $X \geqslant 0 \cdot 4$.

Larger values of w_A and w_B equal to -274 and $-0 \cdot 74$ respectively were therefore selected in order to give a measure of the uncertainty resulting from this discrepancy.

The effect on predictions of the model of this uncertainty has been assessed for discharge of pressurised NH_3 via a 10 m pipe into an atmosphere with temperature 20°C and relative humidity 80%. The results differed little for the two sets of values of w_A and w_B given above. For given mass flux ratios of air and NH_3 the temperature was found to agree to within 1°C, the composition, X, of the aerosol to within $0 \cdot 03$, the quality to within $0 \cdot 002$ and the density relative to air to within $0 \cdot 0003$.

So the model predictions have been found to be surprisingly insensitive to the uncertainty in the parameters of the correlations. However, the temperature for the case considered ranges between -60°C and 20°C while the data incorporated in the recommended vapour pressures of Macriss et al were obtained for $T \geqslant 5$°C. Considerable extrapolation is therefore involved which could lead to greater error in the model predictions than those assessed here. A more detailed investigation of the data is required to quantify this remaining uncertainty.

9. APPENDIX 3

Determination of super-saturation in an ammonia/moist air mixture

It is necessary to know whether a liquid phase exists at all before its composition in the moist air/ammonia mixture can be found. This is done by presuming no liquid phase to exist and then testing to see if the vapour phase is super-saturated.

Let P_1 and P_2 be the partial pressures of water and NH_3 found by presuming no liquid phase to exist. The vapour will be super-saturated if the point $A = (P_1, P_2)$, lies above the saturated vapour pressure curve, shown in Fig. 12.

There are a number of ways of establishing the position of A with respect to the saturated vapour pressure curve as will be seen in Appendix 4. It is convenient in this case to find point B on the saturated vapour pressure curve such that the vapour composition at B is the same as that at point A. From Fig. 12 the equation determining B is

$$\frac{P_1^s(T, X)}{P_1} = \frac{P_2^s(T, X)}{P_2}, \qquad \ldots (A3.1)$$

where X is the molar composition of the liquid phase and the superscript s denotes the saturated vapour pressure. The solution to this equation is unique.

Once X is found, the vapour phase is then found to be saturated if

$$P_1 + P_2 \geqslant P_1^s(T, X) + P_2^s(T, X) \qquad \ldots (A3.2)$$

10. APPENDIX 4

The liquid phase composition in a saturated ammonia/moist air mixture

The equations which determine the liquid phase composition, X, in a saturated mixture are

$$X - \frac{N_{2L}}{N_{1L} + N_{2L}} = 0 \qquad \ldots (A4.1)$$

where, since partial pressures are proportional to molar concentrations, N_{1L} and N_{2L} are found from

$$\frac{N_1 - N_{1L}}{P_1^s} = \frac{N_2 - N_{2L}}{P_2^s} = \frac{N_3}{P_3} \qquad \ldots (A4.2)$$

with

$$P_3 = P_a - P_1^s(T, X) - P_2^s(T, X). \qquad \ldots (A4.3)$$

The method used to solve these equations is to guess a value for X and substitute it in Equations (A4.2), (A4.3) and (A4.4) to find $N_{2L}/(N_{1L} + N_{2L})$ and then to improve the result for X according to the discrepancy in Equation (A4.1).

Unfortunately, the equations have multiple solutions, only one of which is physical (arbitrary values for X can lead to negative values for N_{1L}, N_{2L} or P_3). The range of search for X has to be restricted to eliminate the unphysical solutions. The remainder of this appendix is concerned with finding such a range.

A schematic diagram of the saturated vapour pressure curve at a fixed temperature for ammonia and water is shown in Fig. 13. The solid line gives the total saturated vapour pressure as a function of the liquid phase composition and the dashed line gives the total saturated vapour pressure as a function of the vapour phase composition. Point Z marks the azeotropic mixture (for which the vapour and liquid phases have equal composition). Ammonia and water form a negative azeotrope i.e. Z is at a minimum of $P_1^s + P_2^s$.

It can be shown that this implies the dashed curve must lie below the solid curve. A and B are the points discussed in Appendix 3. Point C lies horizontally to the left of B and point D lies vertically above B. By their construction C and D cannot straddle the azeotrope. (It is assumed here and in the following discussion that B lies to the right of the azeotrope. This however does not affect the substance of the argument. A corresponding argument can be constructed for the alternative case.) It will be shown that the physical solution to the equations lies between the liquid compositions for points C and D.

Consider point C first. We start by considering the supersaturated vapour at point A. Liquid is now assumed to condense with composition equal to that for point C. The combined partial pressure is reduced but, because the NH_3 concentration in the liquid is less than the NH_3 concentration in the vapour, points A, B and C will move to the right. This will continue until the vapour becomes just saturated. The final position for C gives the solution to the equations. The composition at the starting point for C therefore provides a lower bound for X.

It is now shown that N_{1L}, N_{2L} and P_3 are positive at C. The vapour at A is super-saturated and so

$$P_1^s + P_2^s \leqslant \frac{N_1 + N_2}{(N_1 + N_2 + N_3)} P_a. \qquad \ldots (A4.5)$$

This implies that

$$P_1^s + P_2^s \leqslant P_a \qquad \ldots (A4.6)$$

and so P_3 is positive.

Point C was chosen such that

$$\frac{P_1^s}{N_1} = \frac{P_2^s}{N_2} \qquad \ldots (A4.7)$$

and so after eliminating P_2^s from Equation (A4.5), one obtains

$$P_1^s \leqslant \frac{N_1}{N_1 + N_2 + N_3} P_a. \qquad \ldots (A4.8)$$

Since $P_3 = P_a - P_1^s - P_2^s$, Equation (A4.5) gives

$$\frac{P_a}{P_3} \cdot \frac{N_3}{N_1 + N_2 + N_3} \leqslant 1 \qquad \ldots (A4.9)$$

Combining the last two equations gives

$$\frac{N_3 P_1^s}{P_3} \leqslant N_1 \qquad \ldots (A4.10)$$

which, from Equation (A4.2), implies N_{1L} is positive. A similar argument shows that N_{2L} is positive also.

Consider point D now. The final liquid phase composition can never exceed that at D because both the liquid and vapour phases would be richer than the super-saturated vapour without liquid at A. D therefore provides a bound to the right of X. However, the physical region which is known to exist from C to the right does not always extend to D because, when moving to the right from C, N_{2L} and P_3 decrease and may become negative. This occurs whenever A lies below D. A new bound could be found whenever this is so but it is sufficient to ensure that the next guess for X is always to the left of the current guess whenever N_{1L}, N_{2L} or P_3 are found to be less than zero since the physical region is known to extend from C to the right.

11. REFERENCES

1. AKKER, H. E. A. van den and BOND, W. M. Discharge of saturated and superheated liquids from pressure vessels. Prediction of homogeneous choked two-phase flow through pipes. Symposium on the Protection of Exothermic Reactors and Pressurised Storage Vessels. Institute of Chemical Engineers Symposium Series, **85**, pp.91-108 (1984)

2. BATCHELOR, G. K. An introduction to fluid dynamics. Cambridge University Press (1967)

3. BENJAMIN, M. W. and MILLER, J. G. The flow of saturated water through throttling orifices. Trans ASME, **63**, p.419 (1941)

4. BLANKEN, J. M. Behaviour of ammonia in the event of a spillage. Ammonia Plant Safety, **22** (1980)

5. BRODKEY, R. S. The phenomena of fluid motions. Addison-Wesley (1967)

6. BROWN, R. and YORK, L. J. Sprays formed by flashing liquid jets. A.I.Chem.E.J., **8**, pp.149-153 (1962)

7. CREMER and WARNER LTD. Risk analysis of six potentially hazardous industrial objects in the Rijnmond area: A pilot study, Appendix II. D. Reidel (1982)

8. CUDE, A. L. Dispersion of gases vented to atmosphere from relief valves. 1st Int. Loss Prevention Symposium, in The Chemical Engineer, October 1974

9. DUISER, J. A. Escape of liquefied gases from broken pipes. Symposium on the Protection of Exothermic Reactors and Pressurised Storage Vessels. Institute of Chemical Engineers Symposium Series, **85**, pp.163-172 (1984)

10. EDWARDS, A. R. Conduction controlled flashing of a fluid, and the prediction of critical flow rates in a one dimensional system. UKAEA Report AHSB(S) R147 (1968)

11. FAUSKE, H. K. Flashing flows – some practical guidelines for emergency releases. A.I.Chem.E. Symposium, Houston (1985)

12. FLETCHER, B. and JOHNSON, A. E. The discharge of superheated liquids from pipes. Symposium on the Protection of Exothermic Reactors and Pressurised Storage Vessels. Institute of Chemical Engineers Symposium Series, **85**, pp.149-156 (1984)

13. GOLDWIRE, H. C. Jr. Status report on the Frenchman Flat ammonia spill study. 1985 Ammonia Symposium, A.I.Chem.E., Seattle, Washington (1985)

14. HALL, S. F. A simple homogeneous equilibrium critical discharge model applied to multi-component, two-phase systems – the computer programs CRITS and CRITTER. UKAEA Report SRD R127 (1978)

15. HENRY, R. E. The two-phase critical discharge of initially saturated or sub-cooled liquid. Nuclear Science and Engineering, **41**, pp.336-342 (1970)

16. HENRY, R. E. and FAUSKE, H. K. The two-phase critical flow of one-component mixtures in nozzles, orifices, and short tubes. J. Heat Transfer, **93**, pp.179-187 (1971)

17. JONES, M. R. O. and UNDERWOOD, M. C. The small-scale release of pressurised liquefied propane to the atmosphere. Symposium on the Protection of Exothermic Reactors and Pressurised Storage Vessels. Institute of Chemical Engineers Symposium Series, **85**, pp.157-162 (1984)

18. KOESTEL, A., GIDO, R. G. and LAMKIN, D. E. Drop size estimates for a loss of coolant accident. USNRC Report NUREG/CR-1607 (1980)

19. KOOPMAN, R. P. et al. Results of recent large-scale NH_3 and N_2O_4 dispersion experiments. Heavy gas and risk assessment – III, (S. Hartwig ed.), pp.137-156. D. Reidel (1984)

20. LANDAU, L. D. and LIFSCHITZ, E. M. Fluid mechanics. Pergamon Press (1959)

21. LEES, F. P. Loss prevention in the process industries. Butterworths (1980)

22. MacARTHUR, J. G. Ammonia storage tank repairs. Ammonia Plant Safety, **14**, pp.1-5 (1972)

23. MACRISS, R. A. et al. Physical and thermodynamic properties of ammonia/water mixtures. Institute of Gas Technology, Research Bulletin, **34**, Chicago, Illinois (1964)

24. MORRIS, S. D. and WHITE, G. The vapour generation term for flashing flow with particular reference to chlorine and ethylene. Symposium on the Protection of Exothermic Reactors and Pressurised Storage Vessels. Institute of Chemical Engineers Symposium Series, **85**, pp.173-181 (1984)

25. MORTON, B. R., TAYLOR, G. I. and TURNER, J. S. Turbulent gravitational convection from maintained and instantaneous sources. Proc. Roy. Soc. **A234**, pp.1-23 (1956)

26. NYRÉN, K. and WINTER, S. Two phase discharge of liquefied gases through pipes: field experiments with ammonia and theoretical model. 4th International Symposium on Loss Prevention and Safety Promotion in the Process Industries. Institute of Chemical Engineers Symposium Series, **80** (1983)

27. NYRÉN, K. et al. Discharge trials with liquefied ammonia at Simpra, Landstrona, Sweden. Swedish National Defence Research Institute, FOA Report E40009 (1983)

28. OHNESORGE, W. Die Bildung von Tropfen an Düsen und die Auftosung flüssiger Strahlen. Z. angew Math Mech, **16**, pp.335-358 (1936)

29. PERMAN, E. P. Vapour pressure of aqueous ammonia solution, Part I and Part II. Part I, J. Chem. Soc., **79**, pp.718-725 (1901); Part II, ibid, **83**, pp.1168-1184 (1903)

30. PERRY, J. H. Editor. Chemical Engineer's Handbook. McGraw Hill, 6th Edition (1984)

31. PIERRE, B. Total vapour pressure in bars over ammonia-water solutions. Kyltek Tidsk, Sheet 14 (1959)

32. RAMSKILL, P. K. A study of axisymmetric underexpanded gas jets. UKAEA Report SRD R302 (1985)

33. RAYLEIGH, LORD. On the instability of jets. Proc. London Math Soc., **10**, pp.4-13 (1878)

34. REED, J. D. Containment of leaks from vessels containing liquefied gases with particular reference to ammonia. 1st International Symposium on Loss Prevention and Safety Promotion in the Process Industries, The Hague, May 1974, pp.191-195, Elsevier (1974)

35. RESPLANDY, A. Etude expérimentale des propriétés de l'ammoniac (conditionnant les mesures à prendre pour la sécurité du voisinage des stockages industriels). Chimie et Industrie Génie Chimique, **102**, pp.691-702 (1969)

36. RICOU, F. P. and SPALDING, D. B. Measurements of entrainment by axisymmetrical turbulent jets. J. Fluid Mech., **11**, pp.21-32 (1961)

37. SCATCHARD, G. et al. Thermodynamic properties – saturated liquid and vapour of ammonia-water mixtures. Refrig Eng., **53**, pp.413-419, p.446, p.448, p.450 and p.452 (1947)

38. TURNER, J. S. Buoyancy effects in fluids. CUP (1973)

39. WEBER, C. Zum Zerfall eines Flüssigkeitsstrahles. Z angew Math Mech, **11**, pp.136-154 (1931)

40. WHEATLEY, C. J. A theoretical study of NH_3 concentrations in moist air arising from accidental releases of liquefied NH_3 using the computer code TRAUMA. UKAEA Report SRD R393 (1986)

41. WHEATLEY, C. J. A theory of heterogeneous equilibrium between vapour and liquid phases of binary systems and formulae for the partial pressures of HF and H_2O vapour. UKAEA Report SRD R357 (1986)

42. WHEATLEY, C. J., PRINCE, A. J. and BRIGHTON, P. W. M. Comparison between data from the Thorney Island Heavy Gas Trials and predictions of simple dispersion models. UKAEA Report SRD R355 (1986)

43. WUCHERER, J. Measurements of pressure, temperature and composition of liquids and vaporous phase ammonia-water mixtures at saturation point. Z Gesamt Kalte-Ind, **39**, pp.97-104 and pp.136-140 (1932)

44. YOSHINOBU, E. R. A. and SAIMA, A. Turbulent mixing of gases with different densities. JSME, **20**, 139, pp.63-70. (1977).

12. NOMENCLATURE

Variables

A, A_4, A_5, A_6	Cross-sectional area of the flow at various stages downstream.
A_1^0, B_1^0, A_2^0, B_2^0	Constants in the formulae for P_1^0 and P_2^0.
A_1, B_1, A_2, B_2	Functions of X which occur in the formulae for P_1^0 and P_2^0.
C	The concentration of NH_3 in a mixture of NH_3 and moist air.
C_D	The drag coefficient for a rigid sphere.
C_D'	The difference between C_D and Stokes' formula for the drag coefficient of a rigid sphere.
C_{L1}, C_{L2} C_{V1}, C_{V2}, C_{V3}	The specific heat at constant pressure of various pure liquids and vapours.
d_D	The diameter of the largest stable drop at the outlet.
d_5	The diameter of the flow at stage 5.
f	The non-dimensional factor which appears in the most general form of the entrainment equation for a homogeneous momentum jet.
g	Acceleration due to gravity.
G	Total mass flow rate.
G_a	Mass flow rate of air in the jet.
G_6	Mass flow rate of NH_3 at stage 6.
h	Height difference between the pipe inlet and the pipe outlet.
Δh_1, Δh_2	The heat of vapourisation of liquid H_2O and NH_3 respectively.
ΔH	Total change in enthalpy when NH_3 and moist air are mixed together isobarically and brought to equilibrium at some final temperature.
ΔH_1, ΔH_2, ΔH_3, ΔH_{12}	Contributions to ΔH from the mixture components.
L	Length scale which determines the asymptotic decrease in concentration of a homogeneous momentum jet.
$\underline{n}$	A vector parallel to the axis of the outlet.
N_1, N_2, N_3	Number of moles of the components H_2O, NH_3 and air respectively in a mixture of NH_3 and moist air.
N_{1L}, N_{2L}	Number of moles of the liquid phases of H_2O and NH_3 respectively in a mixture of NH_3 and moist air.
P, P_2, P_4	Pressure at various stages downstream.
P_a	Ambient pressure
P_1, P_2	The partial pressures of H_2O and NH_3 in an NH_3/moist air mixture which has no liquid phase.
P_1^0, P_2^0	The saturated vapour pressures of the pure substances H_2O and NH_3 respectively.
P_1^s, P_2^s	The saturated vapour pressures of H_2O and NH_3 above a liquid mixture.
P_3	The partial pressure of air (excluding the moisture component) in an NH_3/moist air mixture.

Q, Q_4, Q_6	The quality (mass fraction of vapour) at various stages downstream.
r_A, r_B	Constants which appear in the formulae for A_1, A_2 and B_1, B_2 respectively.
R	The universal gas constant.
R, R_6	The radius of the jet.
Re_D	The drop Reynolds number.
Re_J	The Reynolds number of the jet at the outlet.
S	The surface over which the momentum flux tensor is integrated.
S_4, S_5, S_{45}	Components of S.
T, T_2, T_4, T_6	Temperature at various stages downstream.
T_a	Ambient temperature.
T_r	The reference temperature at which the heats of vapourisation are evaluated for ΔH.
U, U_4, U_5	The specific internal energy of the two-phase flow at various stages downstream.
U_V	The specific internal energy of the vapour phase.
U_w	The wind speed at the height of the jet.
V, V_4, V_5	The mean axial flow velocity at various stages downstream.
V_D	The terminal gravitational settling velocity at the largest stable drop.
V_i	Components of the flow velocity on S.
w_A, w_B	Constants which appear in the formulae for A_1, A_2, and B_1, B_2 respectively.
We_D	The drop Weber number.
We_J	The Weber number of the jet at the outlet.
X	The molar fraction of NH_3 in the NH_3/H_2O aerosol.
z	Distance along the jet axis from the outlet.
α_J	The jet entrainment coefficient.
α_P	The pipe discharge coefficient.
β	The jet half-angle.
β_∞	The asymptotic jet half-angle.
δ_{ij}	The Kronecker delta, = 1 if i = j, = 0 otherwise.
η	The factor which corrects C_D for motion of the fluid within the drop.
θ	The half-angle of divergence of the flashing flow at the outlet.
Θ	The solid angle subtended by the flashing flow at the outlet.
λ	The ratio of the mean flow speed to the mean axial flow velocity after flashing at the outlet.
μ_L	The viscosity of liquid NH_3.
μ_a	The viscosity of air.
ν, ν_4	The specific volume of the two-phase flow at various stages downstream.
ν_L	The specific volume of liquid NH_3.
ν_V, ν_{V4}	The specific volume of NH_3 vapour at various stages downstream.

v_V^0	The specific volume of pure saturated NH_3 vapour.
Π_{ij}	The momentum flux tensor.
ρ, ρ_6	The density of various stages downstream.
ρ_L	The density of liquid NH_3.
ρ_a	The ambient air density.
σ_L	The surface tension coefficient of NH_3.
φ	The angle between the initial drop trajectory and the horizontal axis of the outlet.

Subscripts

i, j	Components of a vector or tensor.
a	The ambient air.
c	Denotes conditions on the spherical cap after flashing and restoration of thermal equilibrium.
D	Quantities relating to liquid drops at the outlet.
J	Quantities relating to the jet either at the outlet or during entrainment.
L	The liquid phase.
V	The vapour phase.
1, 2, 3, 12	Denotes H_2O, NH_3, air (excluding moisture component), and the H_2O/NH_3 binary liquid phase respectively. In the case of NH_3, the subscript 2 is often dropped for convenience, when no confusion can arise.
2, 4, 5, 6	Denotes various stages downstream (see Fig. 1). These particular numbers are chosen to maintain compatibility with the computer code.
2	In the tank at the height of the outlet from the tank.
4	At the outlet from the pipe.
5	On the equivalent planar surface after flashing and restoration of thermal equilibrium.
6	After rain-out, if any, has occurred but before entrainment of air.

Superscripts

s	Denotes the saturated vapour pressures of H_2O and NH_3 above a binary liquid mixture.
o	Denotes the pure substances H_2O and NH_3.

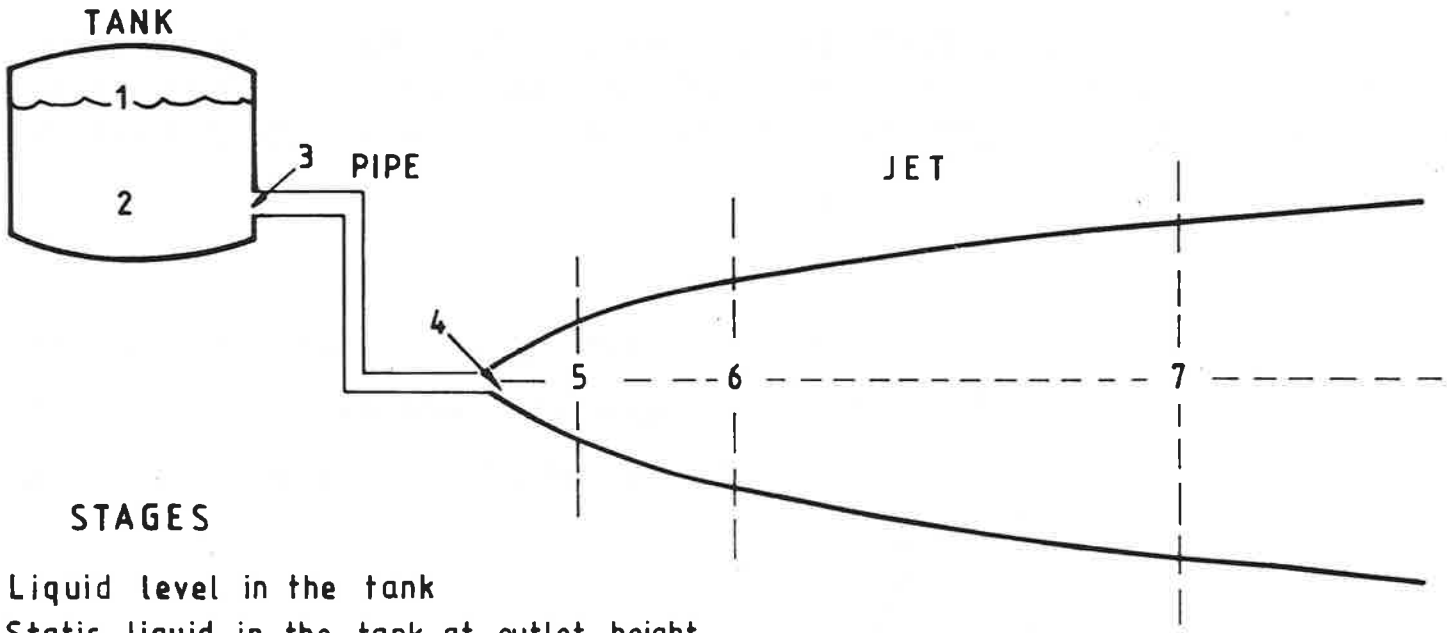

STAGES

1. Liquid level in the tank
2. Static liquid in the tank at outlet height
3. Pipe inlet
4. Pipe outlet
5. Pressure reduced to atmospheric and thermal equilibrium established
6. End of wake entrainment and rain-out
7. End of homogeneous momentum jet entrainment

FIGURE 1

SCHEMATIC DIAGRAM OF THE FLOW PATH FROM THE TANK. THE NUMBERS ASSIGNED TO EACH STAGE ARE USED AS SUBSCRIPTS TO ASSOCIATED VARIABLES USED IN THE TEXT.

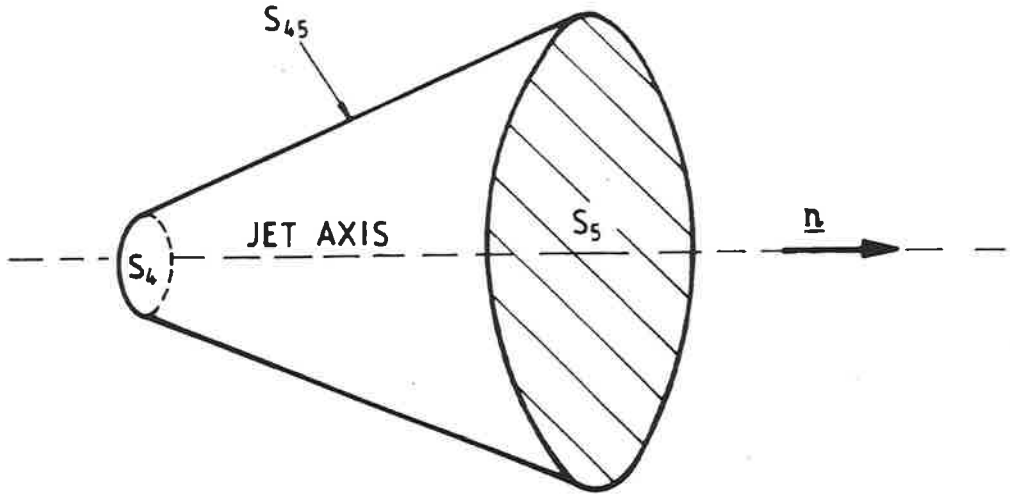

S_4 Surface in plane of outlet from tank or pipe

S_5 Surface downstream over which $P = P_a$ and $T = T_b$

S_{45} Surface over which $P = P_a$ and through which no fluid flows

FIGURE 2

SCHEMATIC DIAGRAM OF FLASHING AT THE OUTLET SHOWING THE SURFACE OVER WHICH INTEGRATIONS ARE DONE TO OBTAIN CONSERVATION LAWS WHICH ENABLE THE FLOW DOWNSTREAM TO BE DESCRIBED.

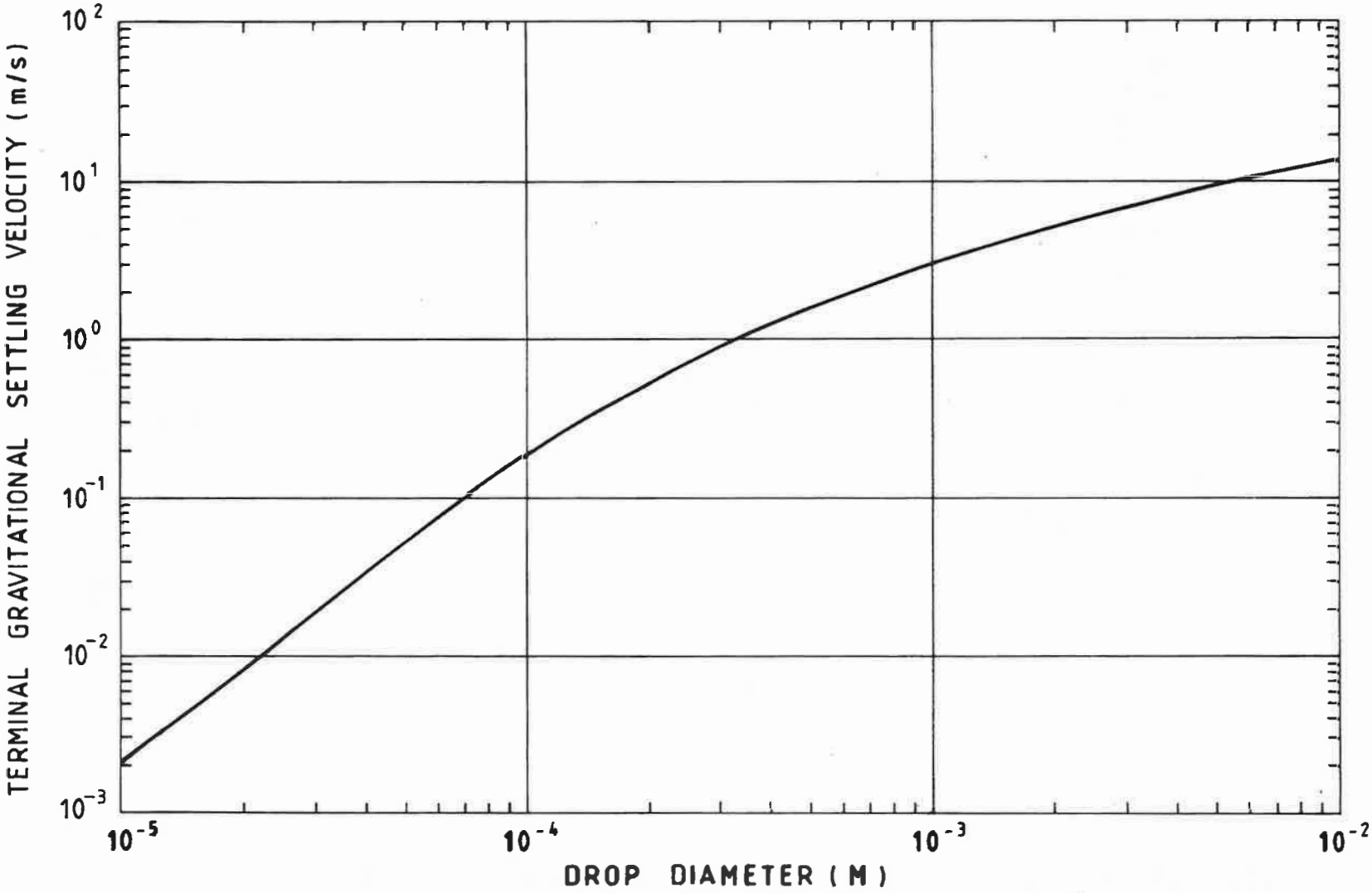
TERMINAL GRAVITATIONAL SETTLING VELOCITY (m/s)
10 2
10 1
10 0
10 -1
10 -2
10 -3
10 -5
10 -4
10 -3
10 -2
DROP DIAMETER (M)

FIGURE 3

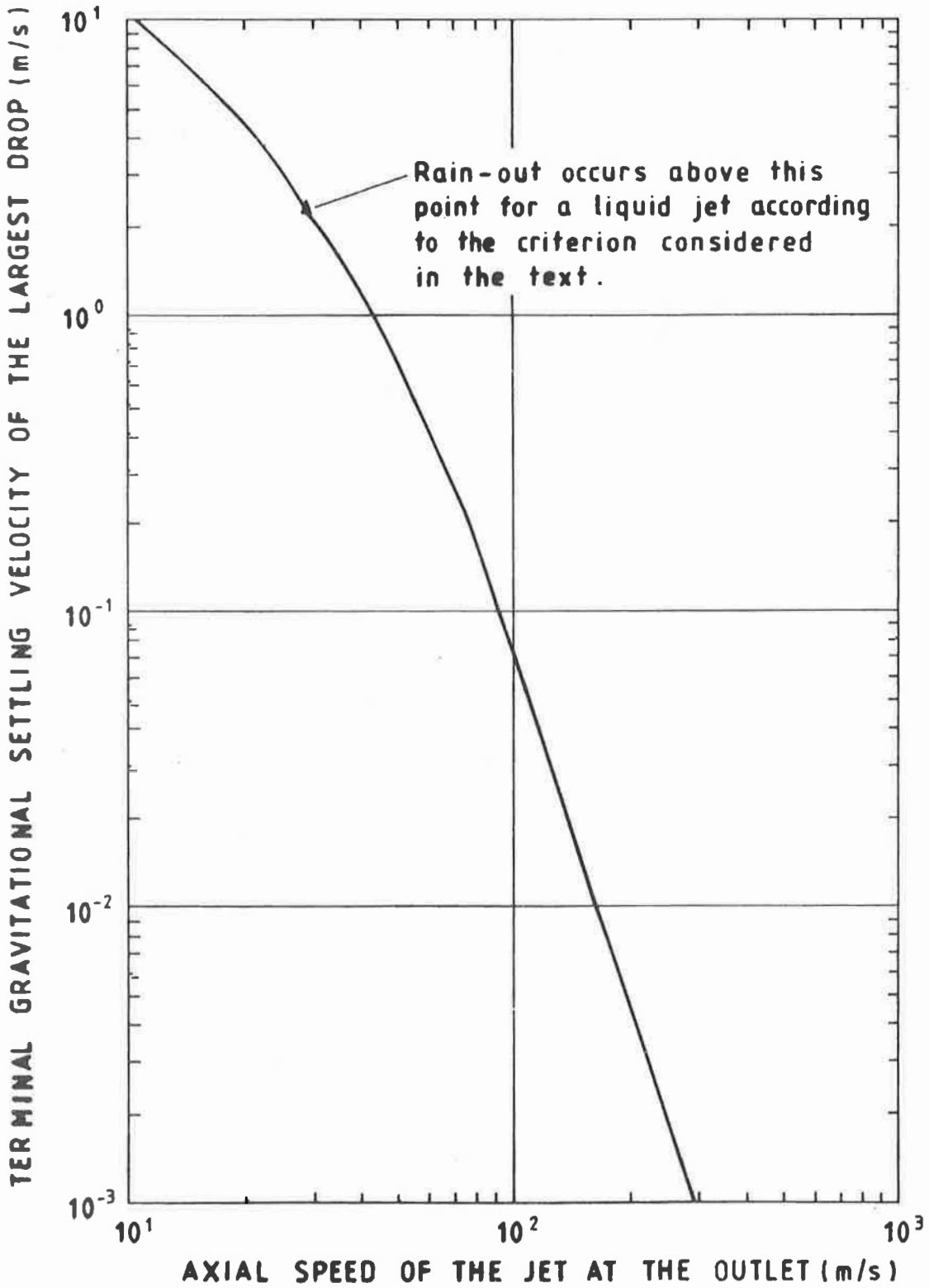
TERMINAL GRAVITATIONAL SETTLING VELOCITY OF THE LARGEST DROP (m/s)
10^{1}
10^{0}
10^{-1}
10^{-2}
10^{-3}
Rain-out occurs above this point for a liquid jet according to the criterion considered in the text.
10^{1}
10^{2}
10^{3}
AXIAL SPEED OF THE JET AT THE OUTLET (m/s)

FIGURE 4

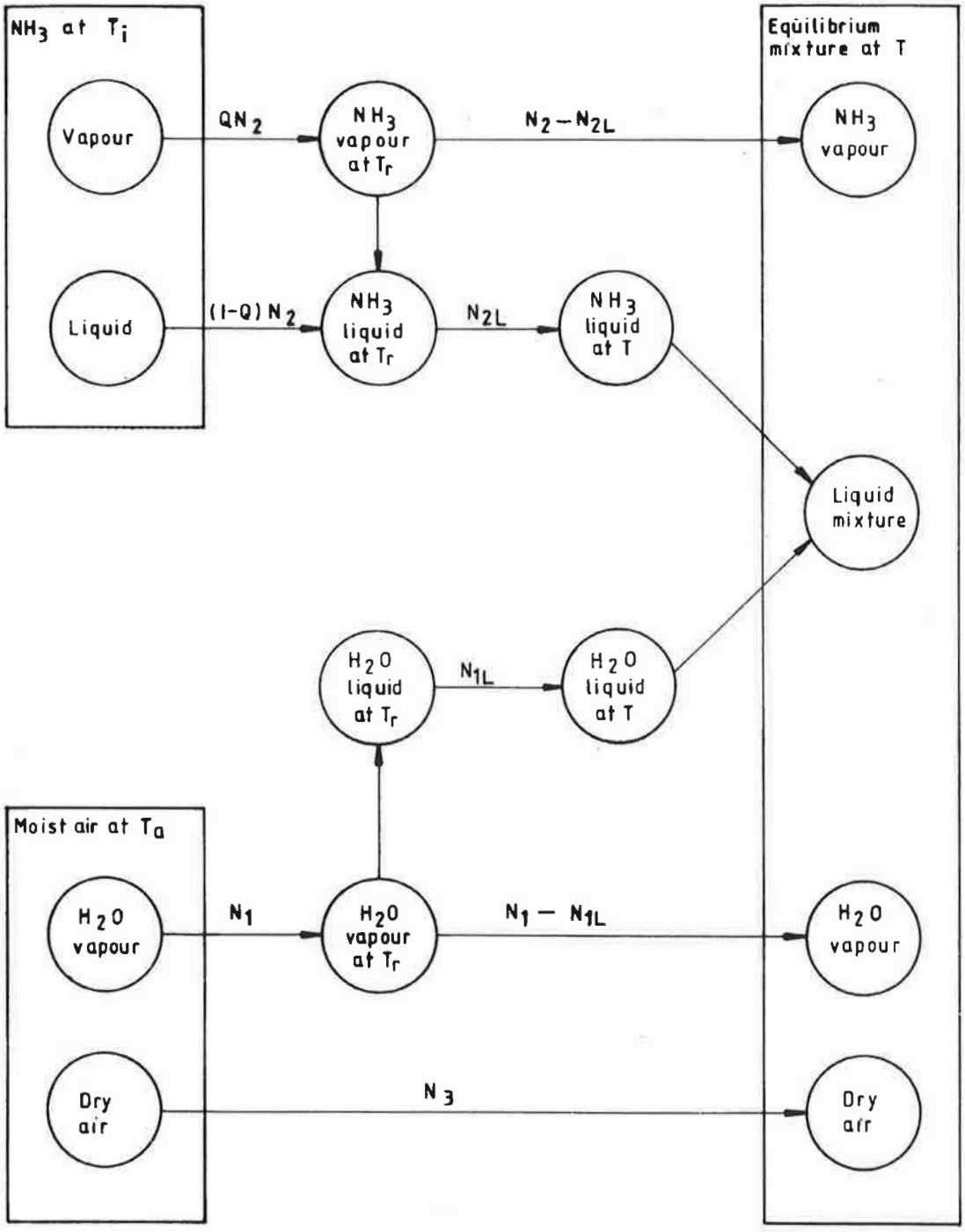

FIGURE 5

THERMODYNAMIC PATHS CHOSEN TO EVALUATE THE CHANGE IN ENTHALPY WHEN MIXING MOIST AIR WITH AMMONIA. THE NUMBER OF MOLES INVOLVED IS SHOWN ABOVE THE ARROWS.

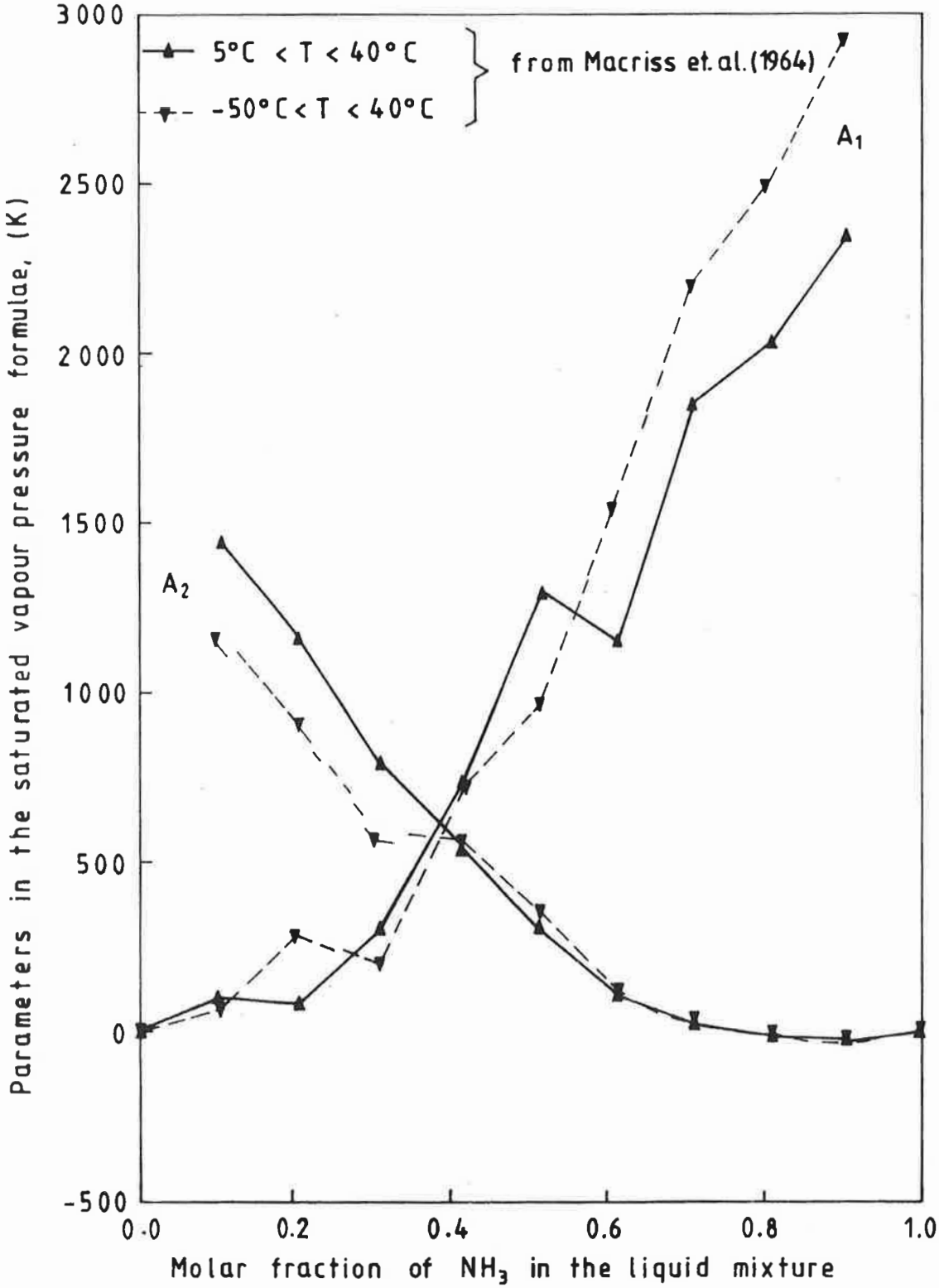
3000
2500
2000
1500
1000
500
0
-500
0.0
0.2
0.4
0.6
0.8
1.0
5°C < T < 40°C
-50°C < T < 40°C
from Macriss et.al.(1964)
A1
A2
Parameters in the saturated vapour pressure formulae, (K)
Molar fraction of NH3 in the liquid mixture

FIGURE 6

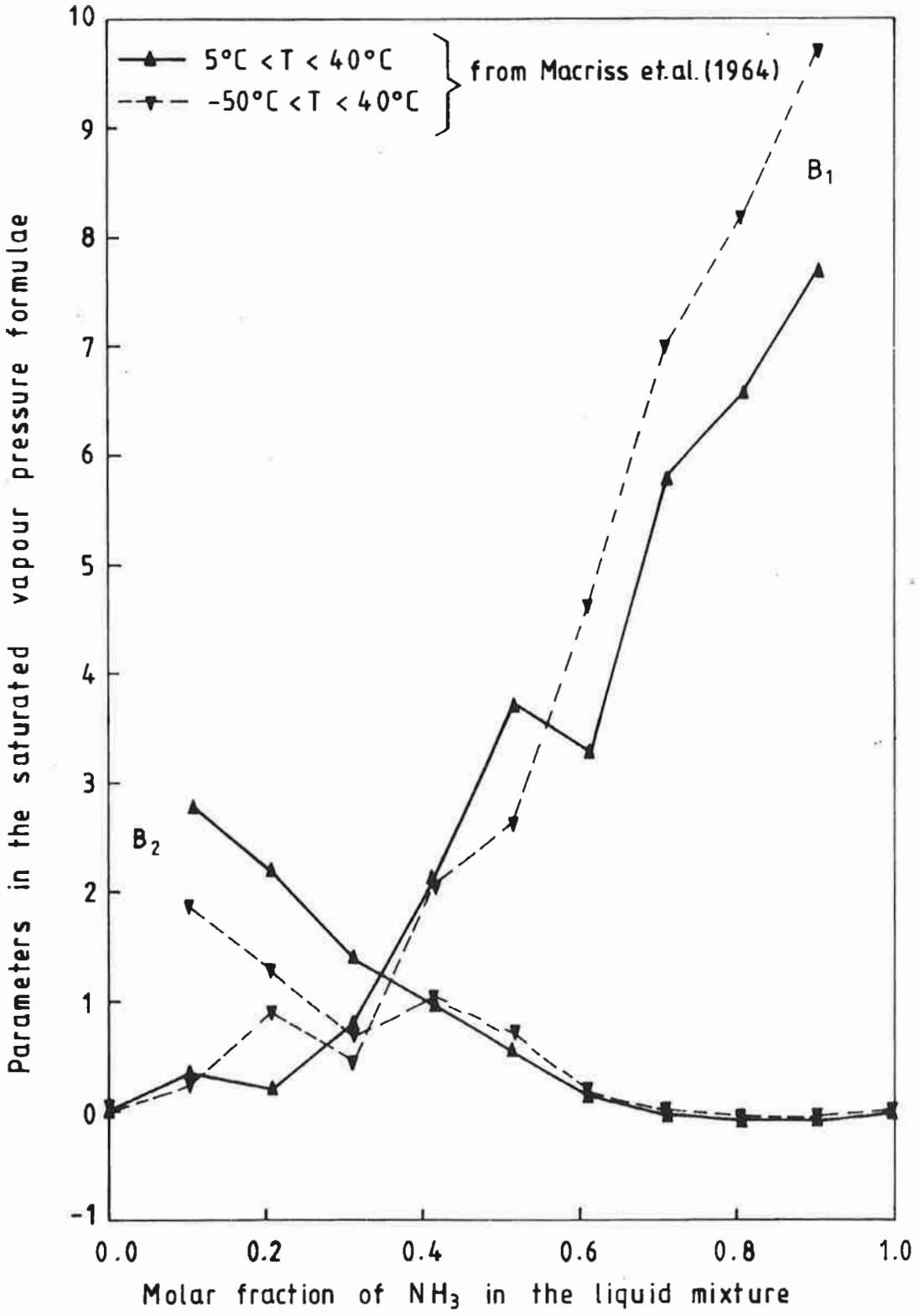
5°C < T < 40°C
-50°C < T < 40°C
from Macriss et.al. (1964)
B1
B2
Parameters in the saturated vapour pressure formulae
Molar fraction of NH3 in the liquid mixture
10
9
8
7
6
5
4
3
2
1
0
-1
0.0
0.2
0.4
0.6
0.8
1.0

FIGURE 7

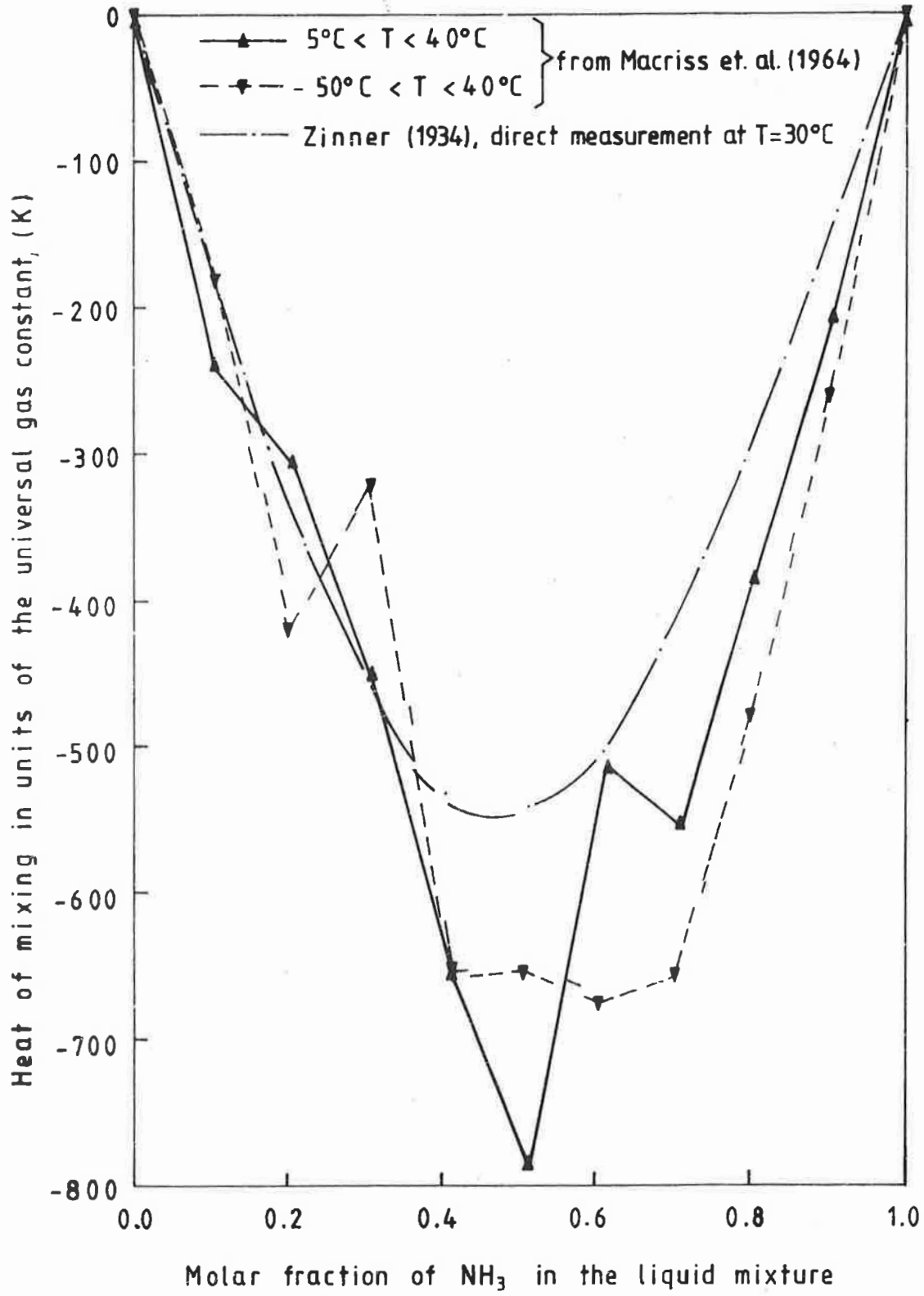
5°C < T < 40°C
- 50°C < T < 40°C
from Macriss et. al. (1964)
Zinner (1934), direct measurement at T=30°C
Heat of mixing in units of the universal gas constant, (K)
0
-100
-200
-300
-400
-500
-600
-700
-800
0.0
0.2
0.4
0.6
0.8
1.0
Molar fraction of NH_3 in the liquid mixture

FIGURE 8

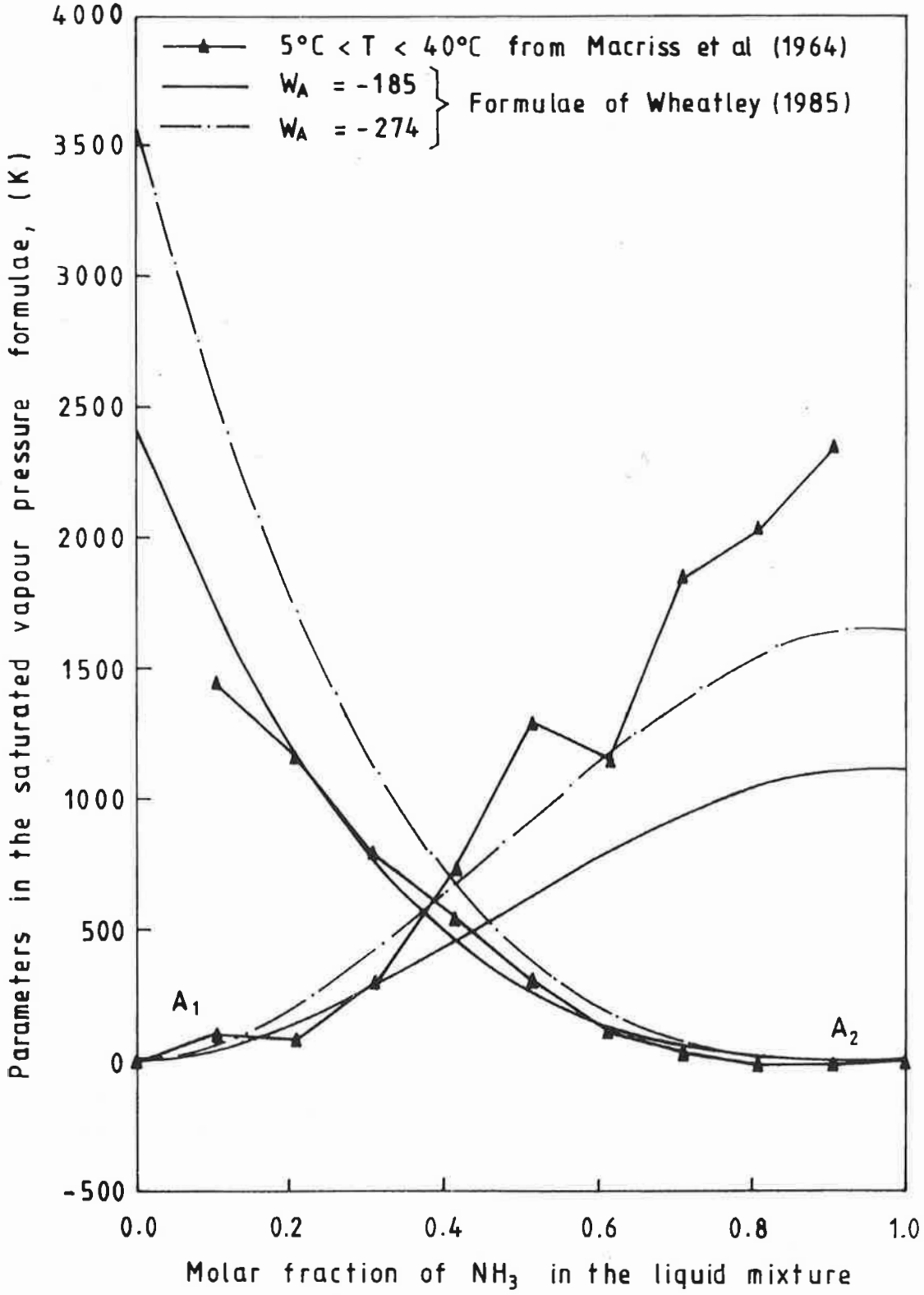
5°C < T < 40°C from Macriss et al (1964)
W_A = -185
W_A = -274
Formulae of Wheatley (1985)
Parameters in the saturated vapour pressure formulae, (K)
4000
3500
3000
2500
2000
1500
1000
500
0
-500
A_1
A_2
0.0
0.2
0.4
0.6
0.8
1.0
Molar fraction of NH_3 in the liquid mixture

FIGURE 9

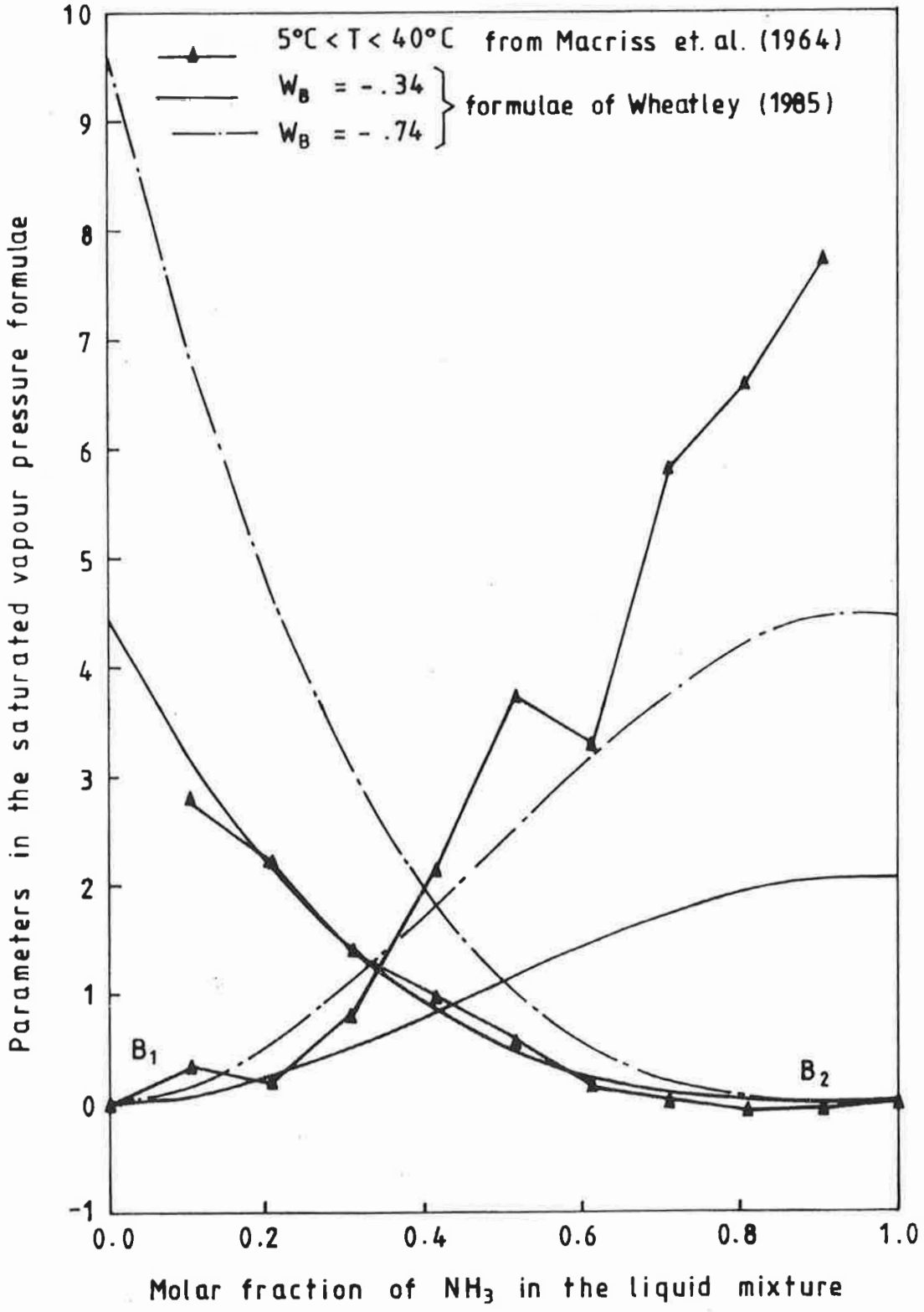
5°C < T < 40°C from Macriss et. al. (1964)
W_B = -.34
W_B = -.74
formulae of Wheatley (1985)
Parameters in the saturated vapour pressure formulae
Molar fraction of NH_3 in the liquid mixture
B_1
B_2
10
9
8
7
6
5
4
3
2
1
0
-1
0.0
0.2
0.4
0.6
0.8
1.0

FIGURE 10

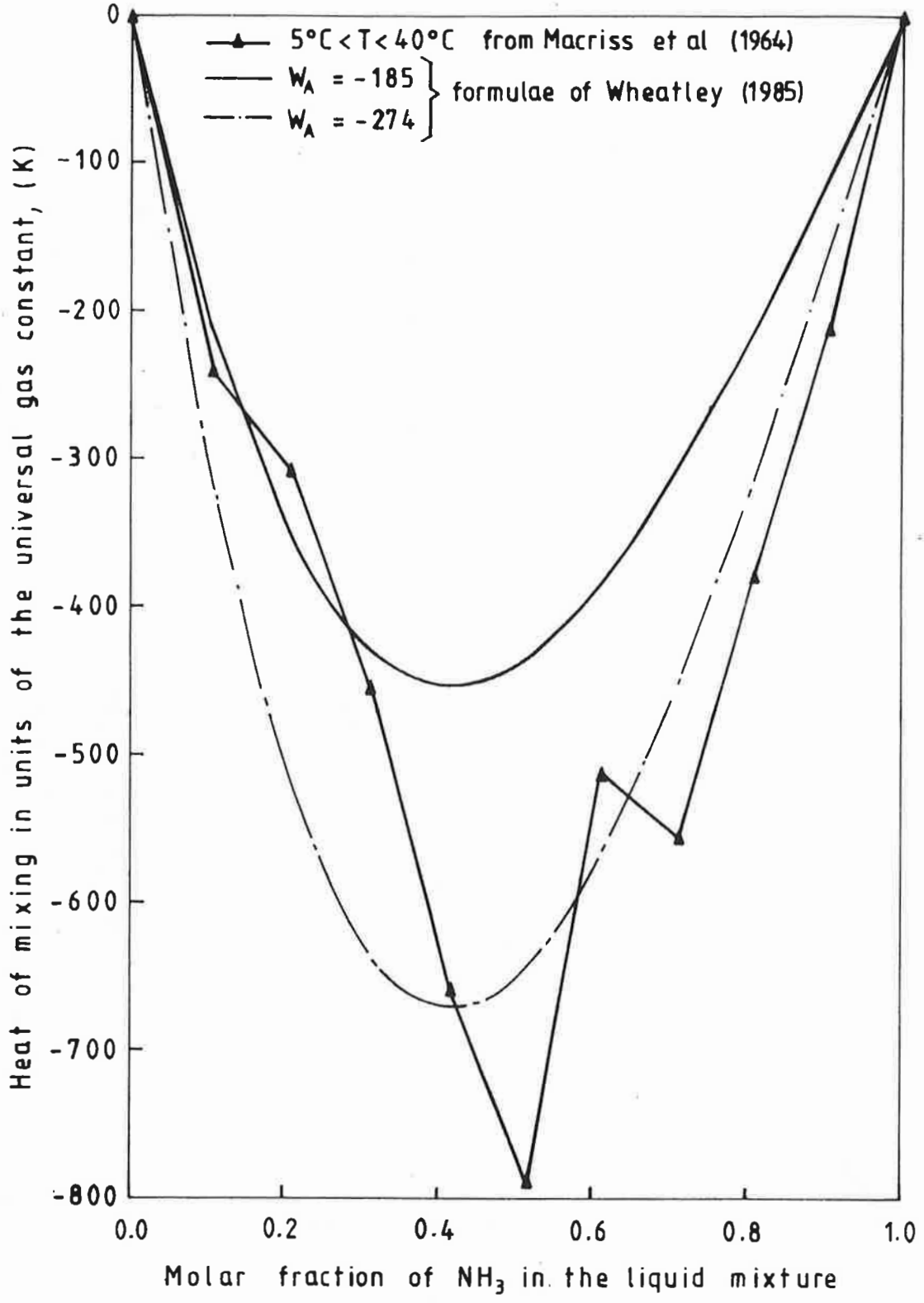
5°C < T < 40°C from Macriss et al (1964)
W_A = -185
W_A = -274
formulae of Wheatley (1985)
Heat of mixing in units of the universal gas constant, (K)
0
-100
-200
-300
-400
-500
-600
-700
-800
0.0
0.2
0.4
0.6
0.8
1.0
Molar fraction of NH_3 in the liquid mixture

FIGURE 11

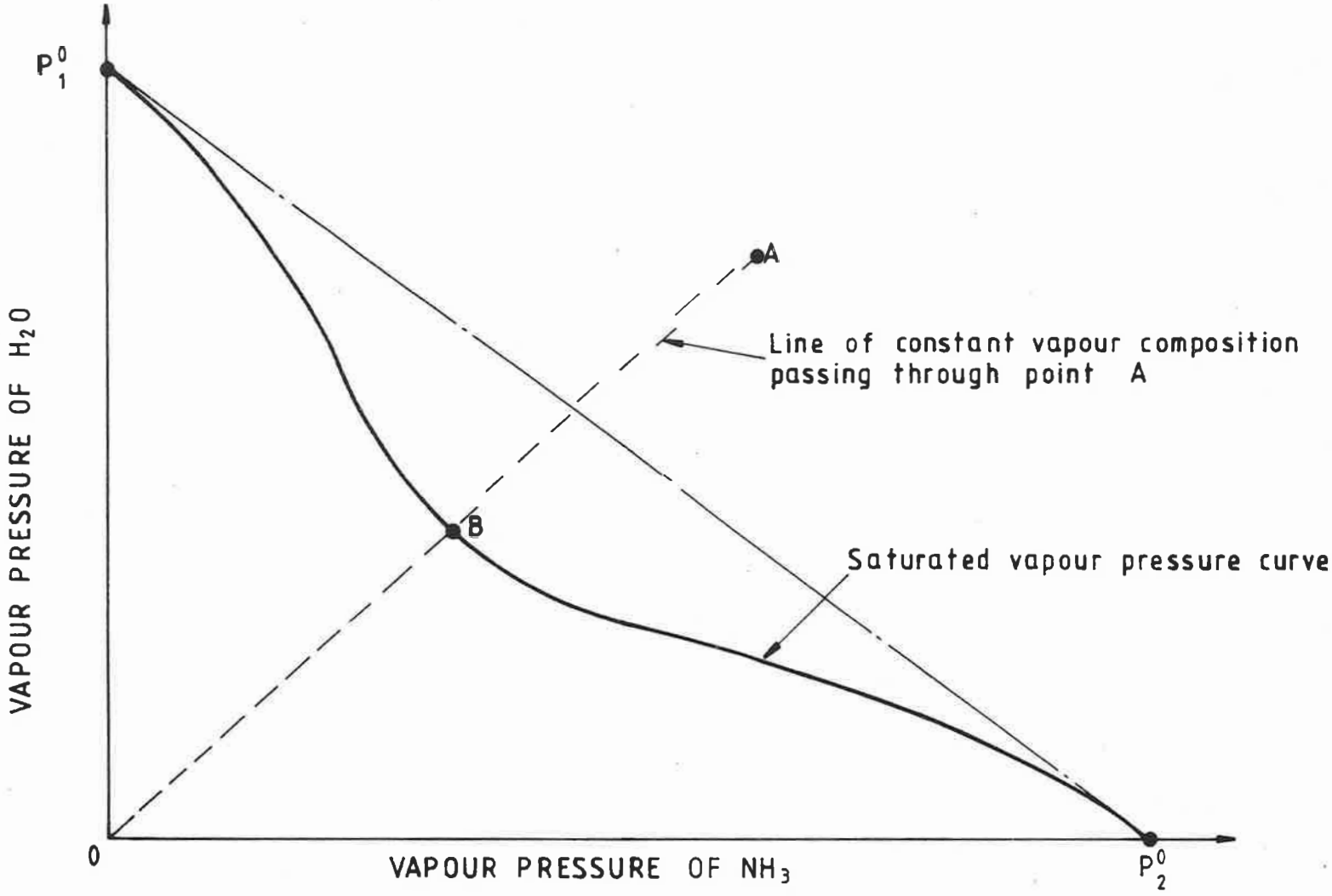

FIGURE 12

SCHEMATIC DIAGRAM ILLUSTRATING THE METHOD USED TO DETERMINE WHETHER AN AMMONIA/MOIST AIR MIXTURE IS SUPERSATURATED

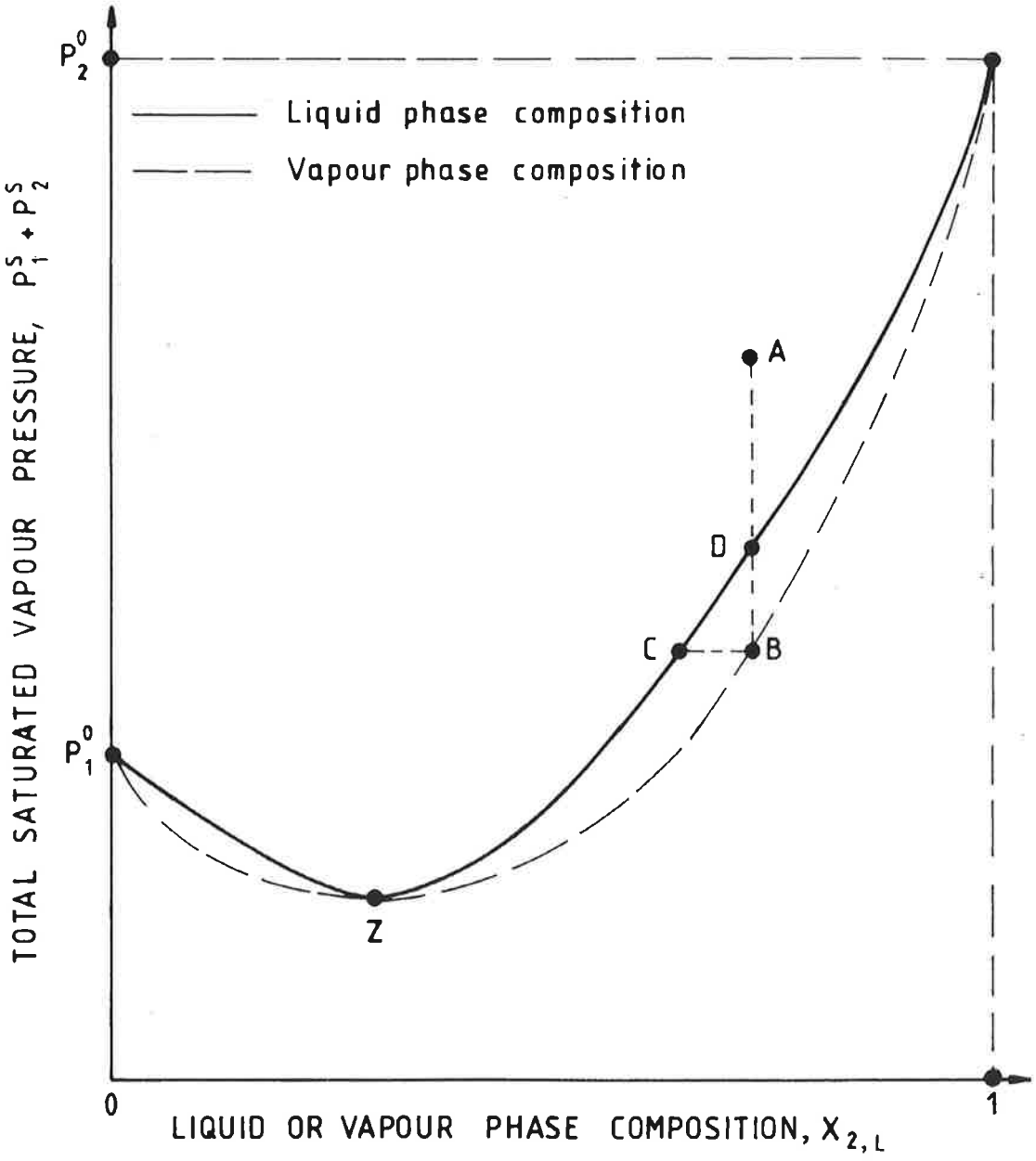

FIGURE 13

SCHEMATIC DIAGRAM OF THE TOTAL SATURATED VAPOUR PRESSURE AT SOME FIXED TEMPERATURE FOR AMMONIA/WATER MIXTURES